

Simplicial closure and higher-order link prediction

Austin R. Benson
Cornell University
arb@cs.cornell.edu

Rediet Abebe
Cornell University
red@cs.cornell.edu

Michael T. Schaub
MIT and University of Oxford
mschaub@mit.edu

Ali Jadbabaie
MIT
jadbabai@mit.edu

Jon Kleinberg
Cornell University
kleinber@cs.cornell.edu

Abstract

Networks provide a powerful formalism for modeling complex systems by using a model of pairwise interactions. But much of the structure within these systems involves interactions that take place among more than two nodes at once—for example, communication within a group rather than person-to-person, collaboration among a team rather than a pair of coauthors, or biological interaction between a set of molecules rather than just two. Such *higher-order interactions* are ubiquitous, but their empirical study has received limited attention, and little is known about possible organizational principles of such structures. Here we study the temporal evolution of 19 datasets with explicit accounting for higher-order interactions. We show that there is a rich variety of structure in our datasets but datasets from the same system types have consistent patterns of higher-order structure. Furthermore, we find that tie strength and edge density are competing positive indicators of higher-order organization, and these trends are consistent across interactions involving differing numbers of nodes. To systematically further the study of theories for such higher-order structures, we propose higher-order link prediction as a benchmark problem to assess models and algorithms that predict higher-order structure. We find a fundamental differences from traditional pairwise link prediction, with a greater role for local rather than long-range information in predicting the appearance of new interactions.

1 INTRODUCTION

Networks are a fundamental abstraction for complex systems and relational data throughout the sciences [2, 15, 43]. The basic premise of network models is to represent the elements of the underlying system as nodes, and to use the links of the network to capture pairwise relationships. In this way, a social network can represent the friendships between pairs of people; a Web graph can encode links among Web pages or topic categories; and a biological network can represent the interactions among pairs of biological molecules or components [10, 14, 22, 43]. But much of the structure in these systems involves *higher-order interactions* between more than two entities at once [8, 23, 39, 44, 64]: people often communicate or interact in social groups, not just in pairs; associative relations among ideas or topics often involve the intersection of multiple concepts; and joint protein interactions in biological networks are associated with important phenomena [41].

These types of higher-order, group-based interactions are apparent even in the standard genres of datasets used for network analysis. For example, coauthorship networks are built from data in which larger groups write papers together, and similarly, email

networks are based on messages that often have multiple recipients. While such higher-order structure is not captured by the topology of a graph, it may be modeled via a collection of formalisms that include set systems [19], hypergraphs [9], simplicial complexes [25], and bipartite affiliation graphs [16, 44]. Despite the existence of mathematical formalisms for higher-order structure, there is no unifying study that analyzes the basic higher-order structure of such datasets. This is in sharp contrast to other notions of “higher-order models” generalizing graph data, such as multiplex networks [29] and higher-order Markov chain models [56, 67], which are successful but still rooted in a pairwise representation paradigm. We study the complementary direction of group interactions, as outlined in the examples above, and use the term “higher-order model” in this sense.

A key reason for the lack of large-scale studies in higher-order models is that data is often collected directly in a network format, thus eliminating higher-order interactions already at the data-collection stage. Another reason is that analyzing higher-order interactions can be computationally challenging for large datasets. Consequently, despite their potential importance, little is known about organizational principles of higher-order structures within real-world datasets. For instance, one question that remains to be answered is whether higher-order interactions enable us to differentiate different kind of datasets, or whether higher-order properties are universal across datasets.

Here, we provide the first steps in the direction of promoting a broad, rigorous study of higher-order topological interactions across domains. To this end, we study the structure and temporal evolution of 19 datasets from a variety of domains that have higher-order interactions. We find that distinct patterns for different domains are immediately revealed with 3-way interaction features that are not available from the graph structure of the networks alone.

Motivated by the importance of triangular structures in network clustering and the theory of triadic closure in social networks [22, 42], we study an extension of this theory via *simplicial closure*, or the way in which groups of nodes evolve until eventually co-appearing in a higher-order structure. In this case, we find that strong previous interactions between subsets of a group increases the likelihood of a *simplicial closure event*, where the nodes appear in a group together. The relative importance of different types of prior interactions depends on the dataset yet remains consistent when considering groups of different sizes for a given dataset. To facilitate future modeling and demonstrate that the higher-order

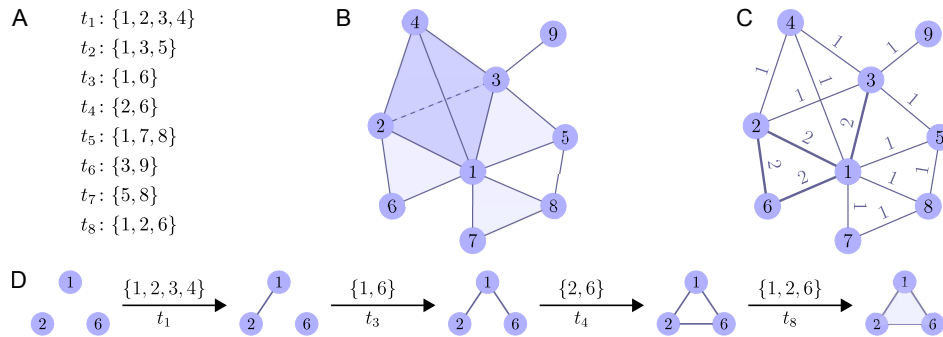


Figure 1: Higher-order network models, open and closed 3-node cliques (triangles), and simplicial closure events. (A) Example higher-order network dataset consisting of eight timestamped simplices on nine nodes. More than one simplex can appear at a given time, which often occurs in real-world data with coarse-grained temporal measurements. We study 19 real-world datasets of this type (Table 1). (B) Visual representation of the dataset (ignoring timestamps). Shading represents the simplices (in order to highlight the difference with traditional graphs), and the dashed line between nodes 2 and 3 denotes three-dimensional perspective for the 4-node simplex $\{1, 2, 3, 4\}$ (this 4-node simplex also has darker shading). Nodes 1, 2, and 3 form a *closed* 3-node clique (i.e., closed triangle) since all three nodes appeared in the same simplex at time t_1 , whereas nodes 1, 5, and 8 form an *open* triangle since all three pairs of nodes co-appeared in a simplex (time t_2 for nodes 1 and 5, time t_5 for nodes 1 and 8, and time t_7 for nodes 5 and 8) but no one simplex contains all three nodes. Thus, the region between nodes 1, 5, and 8 is not shaded. In total, the dataset has seven closed triangles— $\{1, 2, 3\}$, $\{1, 2, 4\}$, $\{1, 3, 4\}$, $\{2, 3, 4\}$, $\{1, 3, 5\}$, $\{1, 2, 6\}$ —and one open triangle— $\{1, 5, 8\}$. We find that the fraction of triangles that are open varies widely depending on the dataset (Figure 2). (C) The “projected graph” of the dataset. The weight of an edge is the number of times its two end points have appeared in a simplex together. Open and closed triangles are both triangles in the projected graph. Traditional network science ideas often ignore higher-order structure and only use this graph. (D) A simplicial closure event for nodes 1, 2, and 6. Each transition lists the new simplex and the time it appears in the dataset. Before closing, the three nodes induce several subgraphs in the projected graph over time. For example, the nodes form an open triangle at time t_4 , which persists until time t_8 when the simplicial closure event occurs. We study properties of such simplicial closure events and predict their future occurrence as part of a framework for evaluating higher-order network models.

patterns are not simple epiphenomena of the underlying link structure, we introduce a higher-order link prediction problem—the forecasting of future higher-order interactions—as an evaluation framework for models and algorithms that aim to predict the emergence of higher-order structure from existing data.

2 STRUCTURAL ANALYSIS OF HIGHER-ORDER NETWORKS

We assembled a diverse collection of 19 datasets, recording the timestamped interactions of groups of entities. Thus, each dataset is a set of timestamped sets of nodes. We call each set of nodes a *simplex*, and the nodes in each simplex take part in a shared interaction at a given timestamp (Figure 1A). For example, in a coauthorship network, a simplex corresponds to a set of authors publishing an article at a given time.

Formally, each dataset consists of N timestamped simplices, $\{(S_i, t_i)\}_{i=1}^N$, where $t_i \in \mathbb{R}$ is the time at which simplex S_i was observed, and S_i is a set representing the nodes in the i th simplex. If $|S_i| = k$, we say that S_i is a k -node simplex.¹ This set-based representation provides a natural format for datasets from a range of domains. We briefly describe our datasets below (see Appendix A for more complete descriptions).

- *Coauthorship data* (coauth-DBLP; coauth-MAG-History; coauth-MAG-Geology): nodes are authors and a simplex is a publication; DBLP spans over 80 years and the other two datasets span about 200 years.
- *Online tagging data* (tags-stack-overflow; tags-math-sx; tags-ask-ubuntu): nodes are tags (annotations) and a simplex is a set of tags for a question on online Stack Exchange forums; the data contains the complete history of the forums.
- *Online thread participation data* (threads-stack-overflow; threads-math-sx; threads-ask-ubuntu): nodes are users and a simplex is a set of users answering a question on a forum; again, the data contains the complete history of the forum.
- *Drug networks from the National Drug Code Directory* (NDC-classes): nodes are class labels (e.g., serotonin reuptake inhibitor) and a simplex is the set of class labels applied to a drug (all applied at one time). (NDC-substances): nodes are substances (e.g., testosterone) and a simplex is the set of substances in a drug; datasets include the complete history of the directory
- *U.S. Congress data* (congress-committees [55]; congress-bills [18]): nodes are members of Congress and a simplex is the set of members in a committee or co-sponsoring a bill; the committees dataset spans 1989 to 2003 and the bills dataset spans 1973 to 2016.

¹Such a structure is called a $(k-1)$ -simplex in algebraic topology, and the set of all its pairs is called a k -clique in graph theory.

Table 1: Summary statistics for our datasets. Each dataset is a collection of timestamped simplices (as in Figure 1).

Dataset	nodes	edges in proj. graph	timestamped simplices	unique simplices
coauth-DBLP	1,924,991	7,904,336	3,700,067	2,599,087
coauth-MAG-Geology	1,256,385	512,0762	1,590,335	1,207,390
coauth-MAG-History	1,014,734	1,156,914	1,812,511	895,668
music-rap-genius	56,832	123,889	224,878	85,429
tags-stack-overflow	49,998	4,147,302	14,458,875	5,675,497
tags-math-sx	1,629	91,685	822,059	174,933
tags-ask-ubuntu	3,029	132,703	271,233	151,441
threads-stack-overflow	2,675,955	20,999,838	11,305,343	9,705,709
threads-math-sx	176,445	1,089,307	719,792	595,778
threads-ask-ubuntu	125,602	187,157	192,947	167,001
NDC-substances	5,311	88,268	112,405	10,025
NDC-classes	1,161	6,222	49,724	1,222
DAWN	2,558	122,963	2,272,433	143,523
congress-bills	1,718	424,932	260,851	85,082
congress-committees	863	38,136	679	678
email-Eu	998	29,299	234,760	25,791
email-Enron	143	1,800	10,883	1,542
contact-high-school	327	5,818	172,035	7,937
contact-primary-school	242	8,317	106,879	12,799

- *Email networks* (email-Enron [30]; email-Eu [49]): nodes are email addresses and a simplex is a set consisting of all recipient addresses on an email along with the sender’s address; email-Enron spans most of the duration of a company’s life-time, and email-Eu spans over 2 years.
- *Contact networks* (contact-high-school [37]; contact-primary-school [61]): nodes are persons and a simplex is a set of persons in close proximity to each other
- *Drug usage in the Drug Abuse Warning Network* (DAWN): nodes are drugs and a simplex is the set of drugs reportedly used by a patient prior to an emergency department visit.
- *Music collaboration* (music-rap-genius): nodes are rap artists; simplices are sets of rappers collaborating on songs.

To provide uniformity across datasets, we restrict to simplices consisting of at most 25 nodes. This is relevant to, e.g., the coauthorship data in which large consortia of hundreds of authors collaborate on a single paper. However, such events are rare and not relevant for our analysis. Table 1 lists some summary statistics of the datasets. The number of unique simplices appearing in the data is minuscule compared to the total number of possible simplices. For example, in the dataset with the smallest number of nodes (email-Enron, 143 nodes), there are nearly 500 million possible simplices of size at most 5, whereas only 1,542 unique simplices appear in the dataset. On the other hand, in most datasets, the number of unique simplices is within an order of magnitude of the number of pairs of nodes that co-appear in some simplex (edges in the projected graph; to be discussed in the next section).

2.1 Higher-order features reveal rich structural diversity

Our data representation distinguishes between the observation of different kinds of k -way interactions between a set of entities. Stated differently, unlike in a graph representation, we do not break down each simplex into a set of (induced) pairwise interactions. Though

the specific representation is not essential provided the information of the group interaction is faithfully encoded, it is convenient to think of our data as an abstract simplicial complex as depicted in Figure 1B.

The simple encoding of the observed information as a graph is called the *projected graph*. Formally, in the projected graph, two nodes are joined by an edge of weight w if they co-appear in w simplices (Figure 1C). A k -clique in the projected graph is a set of nodes among which an edge is present between all pairs. A k -cliques appear if (i) the k nodes were all part of a some simplex, or (ii) each pair was part of some simplex, although all k were never part of the same simplex. In the former case, we say the k nodes form a *closed* clique, while in the latter case we say they form an *open* clique.

We first study the occurrence of open and closed 3-cliques, or triangles (Figure 2). This is the simplest higher-order structure present in our datasets that is not captured by a graph. Furthermore, triangles are one of the most important structural patterns in network analysis [22, 31, 39]. As discussed above, there are two types of triangles which cannot be distinguished by the weighted projected graph alone. In a *closed triangle*, all three nodes have co-appeared in at least one simplex. Formally, $\{u, v, w\}$ is a closed triangle if there exists some simplex S_i for which $\{u, v, w\} \subset S_i$. In an *open triangle*, on the other hand, every pair of the three nodes has co-appeared in at least one simplex, but no single simplex contains all three nodes.

Every simplex with at least three nodes directly creates a closed triangle, while open triangles appear coincidental. Moreover, larger simplices lead to many closed triangles: for instance, a k -node simplex contributes $\binom{k}{3}$ closed triangles. Thus, one might intuit that closed triangles are much more common than open triangles due the presence of (potentially) large groups. On the other hand, only a small fraction of all possible simplices are present in the network when compared to the total number of possible edges in the projected graph, so one might expect that there are more open triangles. Our analysis reveals that, across our datasets, there is a spectrum for the fraction of triangles that are open (Figures 2B and 2C).

While the distribution of simplex sizes is broadly similar in most datasets (Figure 2A), jointly analyzing the edge density in the projected graph with the fraction of triangles that are open reveals a rich landscape of datasets (Figure 2B): (i) low-density with a small fraction of triangles open (coauthorships and music collaboration); (ii) low-density with a large fraction of triangles open (stack exchange threads) (iii) high-density with a large fraction of triangles open (stack exchange tags, contact, bill co-sponsorship); and (iv) high-density with a medium fraction of triangles open (email, Congress committee membership, NDC substances and classes). These results are not skewed by large simplices—the landscape is broadly preserved when restricting to the 3-node simplices (Figure 2D).

Measuring average unweighted degree along with fraction of open triangles also reveals substantial diversity, and datasets from the same domain continue to exhibit similar features (Figure 2C). Restricting the data to only 3-node simplices, we find a near-linear relationship between the fraction of open triangles and the log of the average degree (Figure 2E). A linear model for the data in Figure 2E has $R^2 = 0.85$, compared to $R^2 = 0.38$ for a linear model

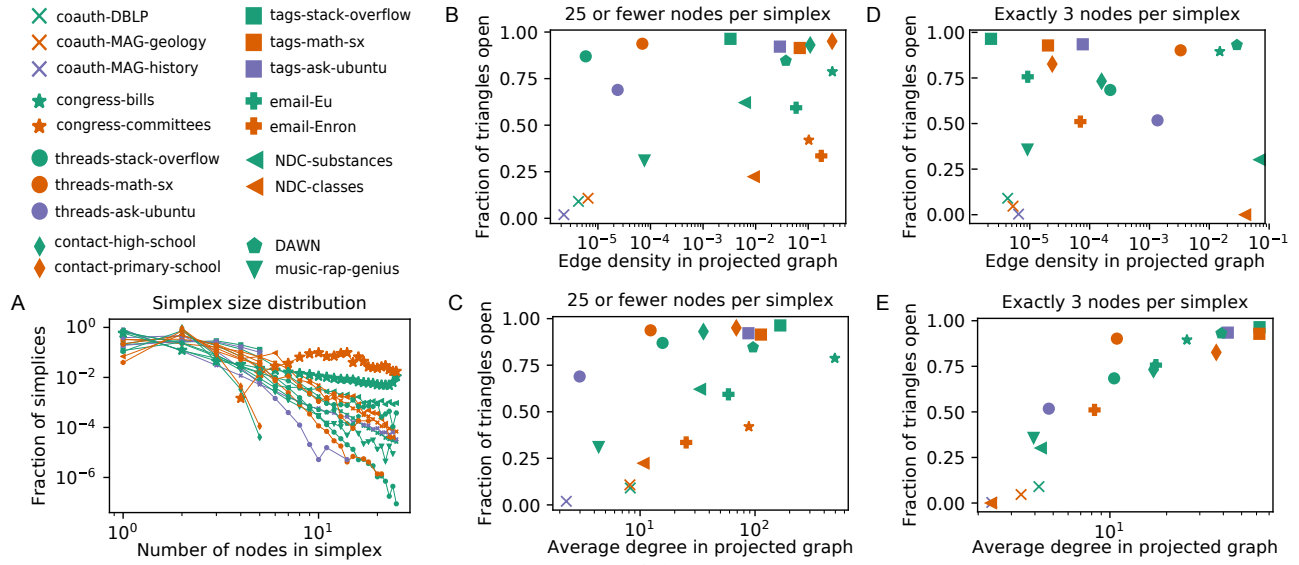


Figure 2: Basic structure of higher-order interaction datasets. (A) Distribution of simplex sizes. In most datasets, small simplices (≤ 4 nodes) are the most common. (B–C) Dataset landscapes in terms of fraction of triangles that are open and either edge density (B,D) or average degree (C,E) when considering simplices with 25 or fewer nodes (B and C) or just 3-node simplices (D and E). Datasets from the same domain tend to be similar with respect to these features, whether or not we include simplices with greater than 3 nodes. Indeed, we can predict the system domain of some datasets by measuring these statistics on egonets (Table 2 and Figure 3).

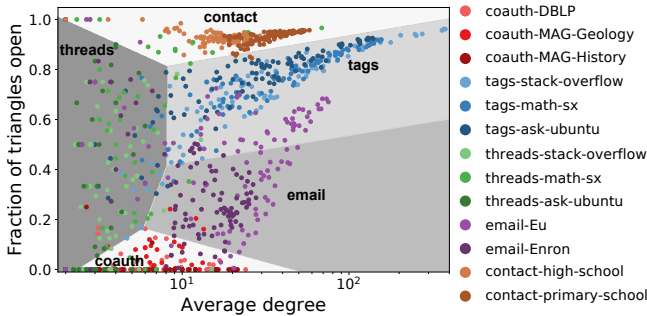


Figure 3: Class decision boundaries of a learned multinomial logistic regression model for predicting five dataset system domains (coauthorship, threads, tags, email, or contact) using the log of the average degree ($\log(\bar{d})$) and fraction of triangles that are open (f) of egonets. Markers correspond to sampled egonets used in model training. The two-feature linear model can predict the 5-class dataset domain with 75% accuracy (Table 2). In conjunction with the prediction accuracies in Table 2, our analysis suggests that the fraction of triangles that are open (a higher-order network statistic) is an important covariate for analyzing and modeling the local structure of higher-order interaction data.

of the data in Figure 2D. This suggests that larger simplices bring diversity to the data.

2.2 Higher-order egonet features discriminate system domains

The structural diversity of the datasets is also present at the local level of egonets (1-hop neighborhoods of nodes), and local statistics can identify the “system domain” of datasets. By system domain, we simply mean the categories identified in Figure 2 that correspond to datasets recorded from the same kind of system. Our collection of datasets has five clear system domains with at least two datasets each: coauthorship, online tags, online thread co-participation, email, and proximity contact.

We trained a multinomial logistic regression model to determine system domain as follows. We computed (i) the fraction of open triangles, (ii) the log of the average degree in the projected graph, and (iii) the log of edge density in the projected graph of 100 egonets sampled uniformly at random (without replacement) from all egonets containing at least one open or closed triangle in each of 13 datasets categorized as coauthorship, stack exchange tags, stack exchange threads, email, or contact. Using 80 samples from each of the 13 datasets as training data, we then trained an ℓ_2 -regularized multinomial logistic regression classifier to predict the system domain using subsets of the three features above and an intercept term. The model was trained using the scikit-learn library (the regularization parameter was set to $C = 10$). Test accuracy was computed on the remaining 20 samples for each dataset. This entire process described was repeated 20 times, resulting in 20 different collections of egonet samples.

The model using the fraction of triangles that are open and log of the average degree as covariates reveals clustering structure of the system domains (Figure 3; the decision boundary comes from

Table 2: Prediction of dataset type by egonet features. For the datasets from coauthorship, threads, tags, email, and contact system domains, we sampled egonets and computed the edge density (ρ), average degree (\bar{d}), and fraction of triangles that are open (f). Using these features, we trained a multinomial logistic regression model to predict the system domain of the network. We report the mean and standard deviation over 20 random samples of 100 egonets. Models incorporating the fraction of triangles that are open outperform the one that does not, highlighting the importance of this feature for higher-order organization. Figure 3 illustrates the model that uses $\log(\rho)$ and f as features.

model features				accuracy	
$\log(\rho)$	$\log(\bar{d})$	f	intercept	random	multinomial LR
X	X	X	X	0.21	0.78 ± 0.02
	X	X	X	0.21	0.75 ± 0.02
X		X	X	0.21	0.60 ± 0.02
X	X		X	0.21	0.49 ± 0.03

one of the 20 samples). This simple model can predict system domain with nearly 75% accuracy, compared to approximately 21% accuracy with random guessing proportional to system domain frequency. The prediction accuracy provides evidence that there are different organizational mechanisms at play locally for different systems. In conjunction with the structure illustrated in Figure 2, this suggests that there is not a single “universal” setting of values for simplicial network statistics; the context of the underlying network matters, but within a given context the parameters are quite stable.

We also trained models with the log of the edge density as a covariate, in addition to the log of the average degree and the fraction of triangles that are open; model accuracy mildly increased from 75% to 78% (Table 2; reported results are the mean and standard deviation over the 20 trials). However, discarding the log of the average degree as a covariate decreases model accuracy to 60%, and only including edge density and average degree without the fraction of triangles that are open decreases model accuracy to 50%. The accuracy numbers are guides in how to model higher-order interaction data. For example, we conclude that the fraction of triangles that are open—a network statistics that relies on knowledge of the higher-order structure in the dataset—is a valuable covariate for identifying system domains. Thus, simple higher-order interactions should be used when analyzing or modeling such data. Furthermore, the average degree tends to be more valuable than edge density when considering local organizational mechanisms.

2.3 A simple generative model for open and closed triangles

We have now seen that there is diversity in datasets from global network statistics and that local statistics reveal system domains of the networks. We now provide a simple generative model of simplices that helps describe how diversity in the datasets might arise. The model uses the hypothesis that 3-node simplices form independently with a fixed probability. While extreme, this hypothesis indeed leads to diversity in the fraction of triangles that are

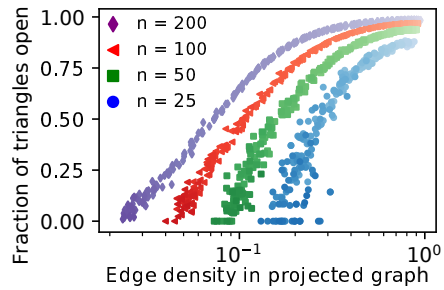


Figure 4: Distribution of the fraction of triangles that are open and edge density in simulations from a model where each triple of n total nodes forms a 3-node simplex independently with probability $p = 1/n^b$, $b \in [0.8, 1.8]$. Color scales with b so that larger p are lighter and smaller p are darker. Varying b creates datasets spanning all possible values of the fraction of triangles that are open.

open. To see this, suppose that a dataset consists only of 3-node simplices on n nodes, and any set of three nodes $\{u, v, w\}$ appears in a simplex with probability $p = 1/n^b$, where $b > 0$ is a parameter regulating the probability of this event. Let X_{uvw} be the indicator random variable that $\{u, v, w\}$ is an open triangle. Then, for large n , it follows from the independence assumption that

$$\mathbb{E}[X_{uvw}] \approx (1 - (1 - 1/n^b)^n)^3. \quad (1)$$

There are two asymptotic regimes here depending on the value of b . If $b < 1$, then $(1 - 1/n^b)^n \leq e^{-n^{1-b}}$, and $\mathbb{E}[X_{uvw}]$ approaches 1 as n gets large. If $b > 1$, on the other hand,

$$\mathbb{E}[X_{uvw}] \approx (1 - (1 - 1/n^b)^n)^3 = O(1/n^{3b-3}). \quad (2)$$

Denote the set of open triangles by \mathcal{O} and the set of closed triangles by \mathcal{C} . According to our calculations above, for large n , the expected number of open triangles is $\mathbb{E}[|\mathcal{O}|] = \sum_{\{u,v,w\}} \mathbb{E}[X_{uvw}] = O(n^3)$ if $b < 1$. For $b > 1$, the expected number of open triangles for large n is $\mathbb{E}[|\mathcal{O}|] = O(n^{3(2-b)})$. The expected number of closed triangles is always $\mathbb{E}[|\mathcal{C}|] = p \cdot \binom{n}{3} = O(n^{3-b})$. Therefore, if $b < 3/2$, the number of open triangles grows faster, and if $b > 3/2$, the number of closed triangles grows faster. To illustrate this numerically, we generated 5 random samples from this model for $b = 0.8, 0.82, 0.84, \dots, 1.8$ and $n = 25, 50, 100, 200$. As suggested by the above theory, the samples have a fraction of open triangles spanning the interval between 0 and 1 (Figure 4).

We can also use the above procedure to construct datasets with a smaller edge density, while keeping the average degree fixed by patching together c replicates of one of these random datasets; this creates a dataset with c times as many nodes, but the same average degree. More formally, if a dataset with n nodes has average degree d and edge density ρ , then the union of c copies of this dataset has cn nodes, average degree d , and edge density $c\rho \binom{n}{2} - n / (\binom{cn}{2} - nc) \approx \rho/c$ (for large n). Thus, our simple independent model spans the two-dimensional feature space in Figures 2B and 2D, but this does not imply that our data was generated by this model.

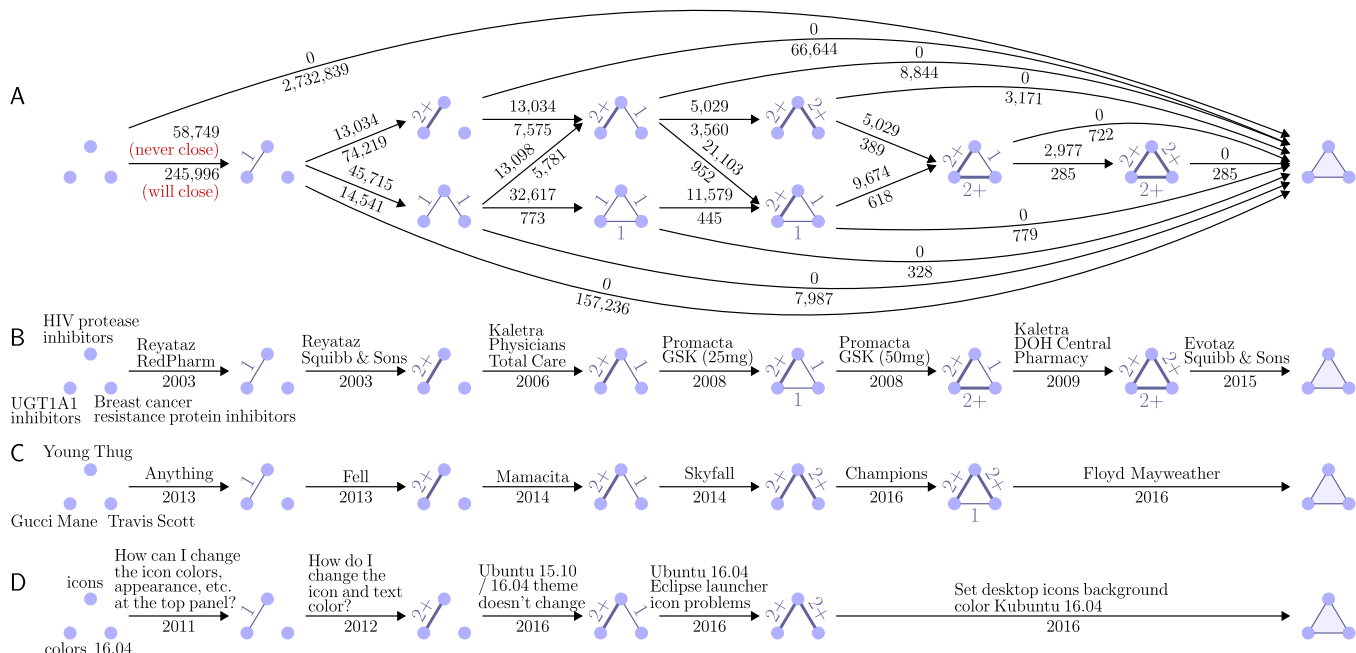


Figure 5: Lifecycles of triples of nodes. Triangle edge weights are from the projected graph binned into weak ties for pairs of nodes appearing in only one simplex together (denoted “1”) and strong ties for pairs of nodes appearing at least two simplices together (denoted “2+”). (A) Lifecycles in the coauth-MAG-History dataset for all triples that eventually form a triangle. Edges represent transitions between configurations, and the numbers are counts of triples that follow the transition. The top number counts triples of nodes that never experience simplicial closure event (i.e., never reach the closed state on the far right), and the bottom number counts triples that do go through a simplicial closure event. (B) Lifecycle of classification codes “HIV protease inhibitors”, “UGT1A1 inhibitors”, and “Breast cancer resistance protein inhibitors” in the NDC-classes dataset, where simplices consist of the labels applied to drugs. Reyataz and Kaletra—two HIV-1 medications—produced strong ties via multiple drug labelers; RedPharm Drug Inc. and E.R. Squibb & Sons, LLC labeled Reyataz, and Physicians Total Care and DOH Central Pharmacy labeled Kaletra. Promacta, a bone marrow stimulant classified as both a breast cancer resistance protein inhibitor and a UGT1A1 inhibitor, creates the open triangle. A strong tie is due to GlaxoSmithKline plc labeling multiple dosages of Promacta as products (25mg and 50mg). The introduction of Evotaz, a combination drug, induces a simplicial closure event for the three labels, 6 years after the open triangle formed. (C) Lifecycle of rap artists Young Thug, Gucci Mane, and Travis Scott. Mane and Thug first collaborated on the song “Anything” on a Mane mixtape; the two subsequently both featured on Waka Flocka Flame’s track “Fell”. Thug then twice featured on Travis Scott’s 2014 mixtape “Days Before Rodeo”, on the tracks “Mamacita” and “Skyfall”. Both Mane and Scott featured on Kanye West’s ensemble track “Champions,” leading to an open triangle. A simplicial closure event occurred when Scott and Mane both featured on Thug’s track “Floyd Mayweather.” (D) Lifecycle of tags “icons”, “colors”, and “16.04” applied to questions on the Ask Ubuntu question-and-answer forum. The tag 16.04 refers to a 2016 Ubuntu release. There are questions about icons and colors independent of the Ubuntu version, dating back to 2011 (just one year after the forum was created). In 2016, users asked 16.04-specific icon questions related to the new release. Finally, a 16.04-specific question on both icons and colors leads to a simplicial closure event.

3 TEMPORAL DYNAMICS AND SIMPLICIAL CLOSURE EVENTS

The above analysis already reveals useful information about the organization of closed and open triangles, and studying the temporal dynamics of the networks in detail offers additional insights. A possible hypothesis for strong prevalence of open triangles would be temporal asynchrony in link creation. For example, consider three Congresspersons u , v , and w in the committee membership dataset, where u is in one committee with v and in another committee with w . If u is not re-elected, there will be no opportunity for the triple

of nodes to form a closed triangle, as u has effectively become inactive. An open triangle may still form if v and w are on the same committee in a future Congress. However, we find that temporal asynchrony does not explain most open triangles. Depending on the dataset, the three edges in 61.1% to 97.4% of open triangles have an overlapping period of activity (including 89.5% for Congress committees; see Appendix B).

Regardless of how open triangles are created, the three associated nodes may of course appear together in a simplex in the future as the network evolves. Deviating from our above simple model of independent creation of closed triangles, we find that many newly formed simplices in our data consist of k nodes that had previously

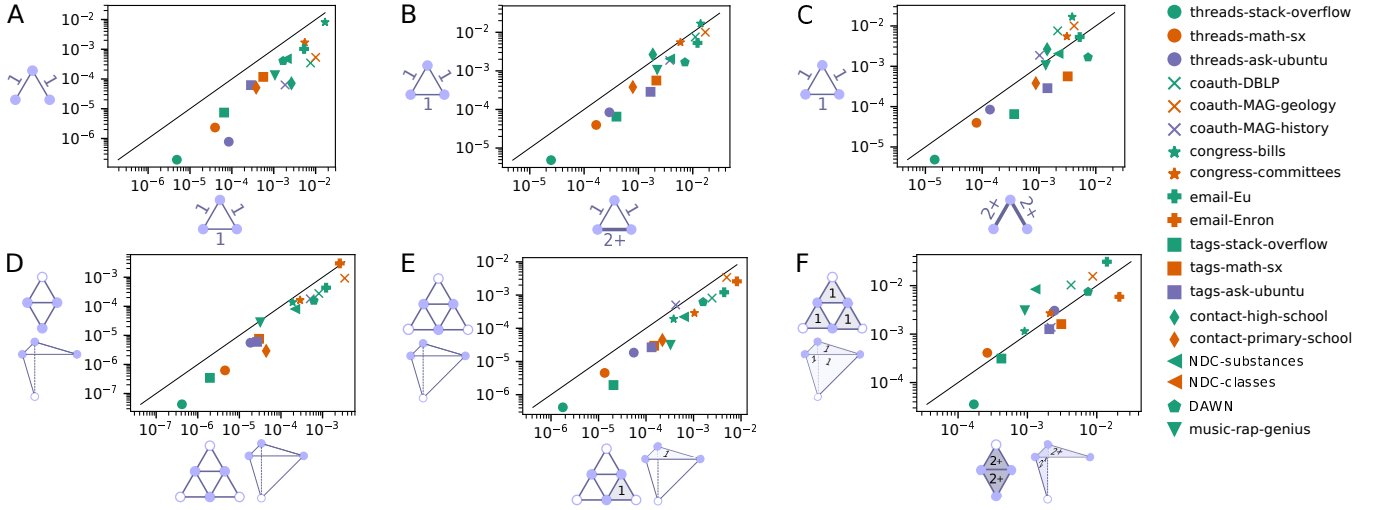


Figure 6: Comparison of simplicial closure event probabilities based on configurations of 3-node and 4-node structures. The simplices appearing in the first 80% of the time spanned by the dataset determine the configuration (appearing as the x-axis and y-axis labels). The scatter plots compare the probability of different configurations going through a simplicial closure event in the final 20% of timestamped simplices. (A–C) Comparison of simplicial closure event probabilities for pairs of 3-node configurations that demonstrate how increasing edge density (A) or tie strength (B) increases the probability of a simplicial closure event. However, the relative importance of edge density and tie strength depends on the dataset (C). (D–F) Comparison of simplicial closure event probabilities for pairs of 4-node configurations. Each axis has two labels giving two pictorial representations of the configuration. The white node in the “flat” representation (left label on x-axis; top label on y-axis) represents the same node, so the 3-dimensional structure can be envisioned by folding the white nodes on top of each other. The other representation (right label on x-axis; bottom label on y-axis) shows a three-dimensional tetrahedral perspective of this folding. We again see that increasing edge density (D) or tie strength (E) increases the probability of a simplicial closure event. Here, “tie strength” is measured at the level of 3-node simplices, i.e., how often three nodes have appeared in a simplex (no times—not shaded; one time—shaded, denoted “1”; or at least two times—shaded, denoted “2+”). The relative importance of edge density and tie strength depends on the dataset but is consistent with the 3-node case. In three of the five datasets for which the configuration on the y-axis in (F) is significantly more likely to go through a simplicial closure event, the open triangle of weak ties is also significantly more likely to close for sets of three nodes (coauth-DBLP, coauth-MAG-Geology, congress-bills; c.f. (C); $p < 10^{-5}$). And in three of the four datasets for which the configuration on the x-axis in (F) is significantly more likely to go through a simplicial closure event the configuration with just two strong ties is also more likely to close than the open triangle with all weak ties (tags-stack-overflow, tags-math-sx, tags-ask-ubuntu; c.f. (C); $p < 10^{-5}$). Moreover, there were no datasets for which tie strength was significantly more indicative of simplicial closure events for one simplex size and density was more important for another (significance level 10^{-5}).

constituted an open k -clique in the projected graph. We say that the appearance of a new simplex containing these k nodes is an instance of a *simplicial closure event*, i.e., the conversion of an open structure to a closed one, as illustrated in Figure 1D.² In the following, we investigate the simplicial closure mechanism as an organizational principle for higher-order interactions.

3.1 Simplicial closure on triangles reveals competing features

Though conceptually similar, three nodes participating in a simplicial closure event is distinct from the well-known phenomenon of *triadic closure events* in social networks [22]. A triadic closure event modifies the structure of the underlying pairwise interactions, whereas a simplicial closure event adds a new higher-order

²Here we are building on terminology for datasets of static sets of simplices [51]. The term “simplicial closure” also appears in the combinatorial topology literature but with a different meaning [?].

interaction without necessarily changing the pairwise structure of the projected graph.

Any induced subgraph on three nodes in the weighted projected graph can change several times before the three nodes appear in a simplex together, i.e., go through a simplicial closure event (Figure 5). We call this the *lifecycle* of the triple of nodes. There are two changes that a triple of nodes can undergo during its lifecycle before a simplicial closure event. First, a new pairwise link can be added between two nodes u and v . This corresponds to an increase in density in this induced subgraph, e.g., the introduction of the drug Promacta adds an edge in Figure 5B. Second, the projected graph edge weight between nodes u and v can increase, which we interpret as an increase in tie strength. For instance, in Figure 5C, the tie strength between Gucci Mane and Young Thug increases after they collaborate on “Fell.” To simplify our analysis, we differentiate only between *weak ties* corresponding to a single interaction

($W_{uv} = 1$ in the projected graph; denoted “1”) and *strong ties* corresponding to multiple interactions over time ($W_{uv} \geq 2$; denoted “2+”). With this binning, there are 11 possible states in a lifecycle (Figure 5A).

To get a first impression of the magnitude of these events, we examine the lifecycle of every triple of nodes that becomes an open or closed triangle in the coauth-MAG-History dataset (Figure 5A). In this dataset, a closed triangle is more likely to have come from a configuration with exactly two strong ties edges (3,171 cases) than from an open triangle ($328 + 779 + 722 + 285 = 2,114$ cases). Most closed triangles are formed by nodes that had no previous interaction (2,732,839 cases); however, since the graph is sparse, the *fraction* of triples of nodes with no prior engagement that go through a simplicial closure event is small (Appendix C). Additionally, if three nodes induce an open triangle with only weak ties at some point in time, then the three nodes are more likely to gain a strong tie before closure (445 cases) than to close directly from that state (328 cases).

We also analyze the probability of a simplicial closure event conditioned on the state of the three nodes in its lifecycle. To do so, we split each dataset based on the temporal order of appearance of the simplices into a training set, consisting of the first 80% of the simplices (in time) and a test set of the remaining 20% of the simplices. Formally, if t_* is the 80th percentile of the timestamps t_1, \dots, t_N , then the training set is the set of timestamped simplices $\{(S_i, t_i) \mid t_i \leq t_*\}$ and the test set consists of $\{(S_i, t_i) \mid t_i > t_*\}$. We then measured the probability that a triple of nodes from the training set is a closed triangle in the test set as a function of its previous configuration in the weighted projected graph, i.e., its lifecycle state in the training data (Appendix D contains all of the simplicial closure event probabilities).

We highlight four important findings. First, the simplicial closure event probability typically increases with additional edges (Figure 6A). In other words, as the edge density of the subgraph induced by the three nodes increases, the probability of a simplicial closure event increases. We formally test this by comparing the closure probability of a fixed weighted induced subgraph configuration and the same configuration with an additional unit-weight edge for all suitable cases. The hypothesis test is conducted as follows. Let n_c and x_c denote the number of instances of an open configuration c in the training set (first 80% of data) and the number of those instances that close in the test set (final 20% of data). For a pair of configurations c and c' , we use a one-sided hypothesis test for $x_c/n_c < x_{c'}/n_{c'}$. We use Fisher’s exact test when $\max(x_c, x_{c'}) \leq 5$; otherwise, we use a one-sample z-test. The additional unit-weight edge configuration has a statistically significant larger simplicial closure event probability in 102 of 113 cases over all datasets and pairs of configurations, whereas the less dense structure is never significantly more likely to close ($p < 10^{-5}$). (Our goal here is to illustrate general trends rather than to find a single statistically significant result.) This result is consistent with both theoretical [22] and empirical [33] studies of dyadic link formation in social networks. However, several of our datasets are not social networks.

Second, the probability of a simplicial closure event typically increases with tie strength (Figure 6B). We test the effect of tie strength by comparing the closure probability of a fixed weighted

induced subgraph containing at least one weak tie, and the same configuration where the weak tie is converted to a strong tie. Increasing the tie strength significantly increases the probability of a simplicial closure event in 82 of 113 cases over all datasets and significantly decreases the closure probability in just 6 of 113 cases ($p < 10^{-5}$). Again, this result is consistent with both theoretical [22] and empirical [3, 31] studies of social networks, even though not all of our networks are social.

Third, neither edge density nor tie strength dominates the likelihood of simplicial closure events (Figure 6C). In the coauthorship and Congress datasets, an open triangle comprised of three weak ties is more likely to close than a 3-node subgraph with just two strong ties. The reverse is true for the stack exchange tags and stack exchange threads datasets. Overall, the open triangle of weak ties is significantly more likely to close than the three nodes with two strong ties in 4 of 19 datasets, whereas the opposite is true in 6 of 19 datasets ($p < 10^{-5}$).

Fourth, the results reveal varying closure dynamics over the dataset domains. In human social interactions, simplicial closure events appear to be driven by a topological form of triadic closure: mutual acquaintance between all the nodes in a set increases the probability of a joint interaction. In contrast, simplicial closure events in the discussion platform networks resemble transitive closure: once there is a sufficiently strong co-occurrences of tags, they become likely to be used together.

A possible concern with our analysis is that we only measured closure probabilities at one point in time for each dataset. Furthermore, while some of our datasets represent a complete history of the network (tags, threads, NDC) and some span a long duration of time (coauthorship, music, congress-bills), a few only contain a slice of the underlying network’s dynamics (email-Eu, contact). However, we find that the closure probabilities and the results on edge density and tie strength are consistent at different points in time (Appendix D).

3.2 Simplicial closure properties extend beyond triangles

All four of the above findings hold for simplicial closure events on four nodes, so our results are not limited to structure on three nodes (Figures 6D to 6F). Now, a simplicial closure event is all four nodes appearing in a simplex, and “tie strength” is measured on 3-node simplices, i.e., how often the 3-node subsets of a 4-node structure have appeared together in a simplex (0, or “open”; 1, or “weak”; at least 2 times, or “strong”).

To measure the effect of edge density, we compare the closure probability of a configuration consisting of a fixed number of edges to the closure probability of the same configuration with an additional edge, keeping the tie strengths fixed (Figure 6D shows one such comparison). In 180 of 228 applicable comparisons over all datasets, the closure probability significantly increases with the edge density and significantly decreases in only 2 cases ($p < 10^{-5}$). To measure the effect of tie strength, we compare the closure probability of a given configuration to the closure probability of the same configuration where the tie strength increases from an open tie to a weak tie or from a weak tie to a strong tie (Figure 6E shows

a case where the tie strength increases from open to weak). The closure probability significantly increases with simplicial tie strength in 26 of 38 cases for 3-edge configurations, 31 of 38 cases for 4-edge configurations, 77 of 114 cases for 5-edge configurations, and 177 of 359 cases for 6-edge configurations; compared to a significant decrease in closure probability in just 2 of 38, 1 of 38, 1 of 114, and 4 of 359 cases ($p < 10^{-5}$). Therefore, tie strength is also a positive indicator of simplicial closure in 4-node configurations.

There is also tension between the influence of sparser configurations with strong ties and denser configurations with weak ties. Figure 6F shows one such comparison. In this case, three out of five datasets for which edge density is significantly more indicative than tie strength in the 3-node comparison of Figure 6C, edge density is also significantly more important in the 4-node case ($p < 10^{-5}$). And in three of the four datasets for which tie strength is significantly more indicative than edge density in the same 3-node case, the same is true in the 4-node case. Finally, there is no dataset for which tie strength was significantly more influential for one simplex size and density was significantly more influential for another.

4 HIGHER-ORDER LINK PREDICTION

Thus far, we have showed that higher-order interactions provide a rich source of additional information beyond traditional network modeling. Our analysis leaves open many questions, such as the development of better mechanistic models for the emergence of these interactions. To facilitate this process, we propose an analog of link prediction for higher-order structure.

4.1 Model evaluation framework

The basic premise in link prediction—whether pairwise or higher-order—is to use structural network properties up to some time t to predict the appearance of new interactions after t . In traditional network analysis, link prediction is a cornerstone problem and a highly successful evaluation framework for comparing different models via a well-calibrated prediction task [34, 36]. Specifically, link prediction examines data that evolves over time and sees how well a given model predicts the appearance of new links—for example, new coauthorships appearing in a coauthor network, or new messages between pairs of people in an email network.

In this context, a *model* is interpreted broadly and may be mechanistic (e.g., preferential attachment [7]), statistical (e.g., probabilistic hierarchical models [12]), or implicitly encapsulated by a principled heuristic algorithm. For instance, personalized PageRank is a model capturing the fact that a large number of walks between two nodes drives up the connection probability between them [34]. A key advantage of link prediction as an evaluation framework is precisely that it can handle these various kinds of models. This holds even in the absence of a likelihood expression, which would be required for a more standard statistical evaluation of goodness of fit. While ultimately we may want to arrive at a generative, causal description of the emergence of higher-order patterns, the flexibility of link prediction enables us to probe the importance of features of the network data in a simple manner without having to create a formal statistical model.

Link prediction has proved valuable both for methodological reasons and also in concrete applications. Methodologically, asking whether one model is better than another at predicting new links provides a data-driven way of assessing the effectiveness of the models [24, 34, 57]. Link prediction also has a number of direct applications that cut across disciplines, including predicting friendships in social networks [4], inferring new relationships between genes and diseases [66], and suggesting novel connections in the scientific community [63].

Link prediction is also used within model selection tools for evaluating community detection algorithms [20, 28]. In these cases, link prediction may be interpreted as the smallest possible test for the fit of a model as we need to predict only one edge at a time. However, if one were to consider all edges in a cross-validation assessment, good link prediction performance indicates a good model fit for other structure in the data. Our higher-order link prediction task probes a larger set of features, in that it requires us to be able to predict more aspects of the data (any higher-order interaction, in principle).

For simplicity of presentation and scalability reasons, we predict simplicial closure events on triples of nodes. Thus, the higher-order link prediction problem examined here is predicting which triples of nodes that have not yet appeared in a simplex together will be a subset of some simplex in the future. Our above analysis suggests that open triangles or triples of nodes with strong ties are the most likely to close in the future. For our experiments, we predict which open triangles will go through a simplicial closure event in the future. Thus, this is a problem completely ignored by traditional link prediction, which would just view the triangle as already part of the graph. From a computational view, this restriction also makes it feasible to enumerate all open structures upon which the algorithms will make a prediction, using only modest computational resources. Thus, we avoid a common problem in link prediction of how to pare down an enormous candidate set of potential links, which itself is an active research topic [6, 59].

4.2 Simple local features predict well

We first split the data into training (first 80% of simplices in time) and test (final 20%) sets. Then, we evaluated the prediction performance of several new models (several inspired from classical link-prediction) on each dataset by the area under the precision-recall curve (AUC-PR) metric (Table 3). AUC-PR is appropriate for prediction problems with class imbalance [13], which is the case for our datasets. We use random scores as a baseline, which, with respect to AUC-PR, corresponds to the proportion of open triangles in the training set that go through a simplicial closure event in the test set.

We compare eight models here and provide additional comparisons in Appendix F. Three are heuristics based on our finding that tie strength is indicative of closure; these are the harmonic, geometric, and arithmetic means of the three edge weights in the open triangle. Two more are based on the Adamic-Adar model [1] and the preferential attachment model. The latter has been suggested as a growth mechanism of coauthorship networks [7, 42]. Two are based on longer path counts (Katz and personalized PageRank), which are models known for providing good prediction in dyadic

Table 3: Open triangle closure prediction performance based on eight models: harmonic, geometric, and arithmetic means of the 3 edge weights; 3-way Adamic-Adar coefficient; preferential attachment; Katz similarity; personalized PageRank similarity (PPR); and a feature-based supervised logistic regression model. Performance is AUC-PR relative to the random baseline, i.e., relative to the fraction of open triangles that close. The top performance number for each dataset is bolded.

Dataset	Harm. mean	Geom. mean	Arith. mean	Adamic-Adar	Pref. Attach	Katz similarity	PPR	Logistic Regression
coauth-DBLP	1.49	1.59	1.50	1.60	0.74	1.51	1.83	3.37
coauth-MAG-History	1.69	2.72	3.20	5.82	2.49	3.40	1.88	6.75
coauth-MAG-Geology	2.01	1.97	1.69	2.71	0.97	1.74	1.26	4.74
music-rap-genius	5.44	6.92	1.98	2.10	2.15	2.00	2.09	2.67
tags-stack-overflow	13.08	10.42	3.97	6.63	2.74	3.60	1.85	3.37
tags-math-sx	9.08	8.67	2.88	6.34	2.81	2.71	1.55	13.99
tags-ask-ubuntu	12.29	12.64	4.24	7.51	5.63	4.15	2.54	7.48
threads-stack-overflow	23.85	31.12	12.97	3.19	3.89	11.54	4.06	1.53
threads-math-sx	20.86	16.01	5.03	23.32	7.46	4.86	1.18	47.18
threads-ask-ubuntu	78.12	80.94	29.00	30.82	6.62	32.31	1.51	9.82
NDC-substances	4.90	5.27	2.90	5.97	4.46	2.93	1.83	8.17
NDC-classes	4.43	3.38	1.82	0.99	2.14	1.34	0.91	0.62
DAWN	4.43	3.86	2.13	4.77	1.45	2.04	1.37	2.86
congress-committees	3.59	3.28	2.48	5.04	1.31	2.59	3.89	7.67
congress-bills	0.93	0.90	0.88	0.66	0.55	0.78	1.07	107.19
email-Enron	1.78	1.62	1.33	0.87	0.83	1.28	3.16	0.72
email-Eu	1.98	2.15	1.78	1.37	1.55	1.79	1.75	3.47
contact-high-school	3.86	4.16	2.54	2.00	1.13	2.53	2.41	2.86
contact-primary-school	5.63	6.40	3.96	3.21	0.94	4.02	4.31	6.91

link prediction [34]. Lastly, we use a supervised logistic regression model based on features from the other models.

No single model performs the best over all datasets, but our proposed baseline algorithms can achieve much better performance than randomly guessing which open triangles go through a simplicial closure event. In the threads datasets, we achieve between one and two orders of magnitude performance improvements with the harmonic and geometric means, which indicates that local tie strength is relatively more important for these datasets than others. The absolute performance of the algorithms is far from perfect (see Appendix F), as the higher-order link prediction is challenging. This finding is consistent with recent research on subgraph prediction in pairwise networks [38]. However, our goal here is to identify some of the important structural features of the problem, rather than to predict with perfect accuracy.

The harmonic and geometric means of edge weights perform well across many datasets, which further highlights the importance of tie strength in predicting simplicial closure events. This finding is fundamentally different from traditional link prediction with pairwise interactions (i.e., for the edges in a graph). In traditional link prediction, a key principle is that it is valuable to use information contained in paths of non-trivial length between two nodes u and v for predicting a link between them—for example, PageRank and Katz measures are effective [34, 36]. In this sense, higher-order link prediction is fundamentally more local in its overall structure. This arises from the ability of a k -tuple of nodes, for $k \geq 3$, to contain rich local information in its interactions among subsets of size $k - 1$, a phenomenon that has no natural analogue when $k = 2$.

The arithmetic mean performs the worst of the three means in all but one dataset. We further analyze the performance of edge

weight means using the generalized mean with parameter p as score functions: $s_p(u, v, w) = [(W_{uv}^p + W_{uw}^p + W_{vw}^p)/3]^{1/p}$, where W_{ab} is the weight between nodes a and b in the projected graph. The harmonic, arithmetic, and geometric means are the special cases where $p = -1$, $p = 1$, and the limit $p \rightarrow 0$. Generally, prediction performance is (i) unimodal in p , (ii) maximized for $p \in [-1, 0]$, and (iii) better for $p < -1$ than for $p > 1$ (Figure 7). Two exceptions are NDC-classes and coauth-MAG-History. The former is the only dataset without an open triangle with exactly one strong tie to close. Thus, smaller p should perform better, as this accounts more for the minimum edge weight value. The latter is the dataset with the smallest average degree in the projected graph (Figure 2C). Therefore, a single strong edge could provide the signal for closure, in which case a larger p is a better score function.

The supervised learning approach also performs well broadly, especially in the larger datasets such as the coauthorship datasets, which have sufficient training data to learn a good model. However, even when including the features of the other models, the method does not always perform the best. This is likely a case of overfitting. In the case of the Congress bills data, the supervised method captures a unique feature of this dataset—nodes appearing in fewer simplices are *more* likely to go through a simplicial closure event. This is possibly due to the ambition of junior Congresspersons. The fact that combinations of features prove effective in many domains highlights the richness of the underlying problem, and the array of methods and findings presented here can guide progress on better models.

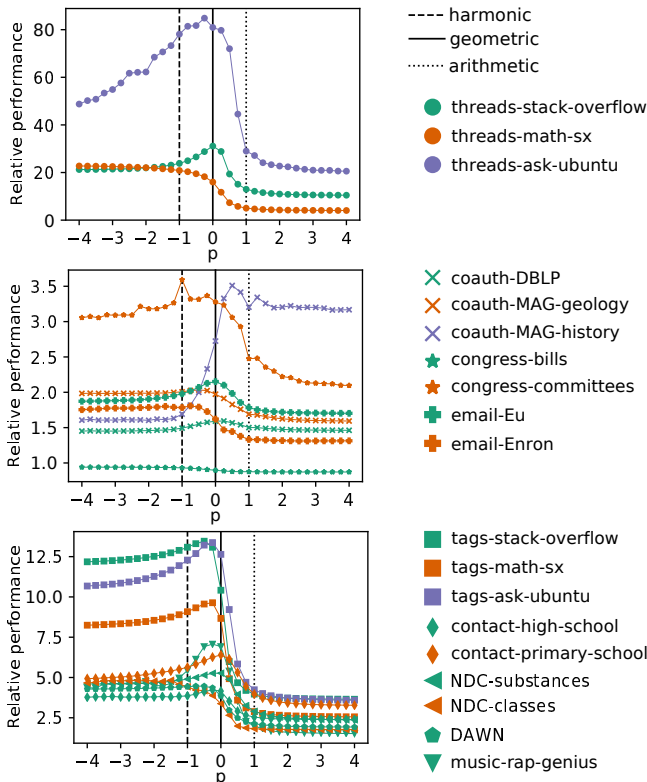


Figure 7: AUC-PR relative to random predictions as a function of the parameter p in the generalized mean heuristic model for higher-order link prediction.

5 DISCUSSION

The dyadic network modeling paradigm has been successful but fails to capture natural higher-order interactions. Here, we established the foundation for analyzing the basic structure of temporal networks with higher-order structure. We found rich structural variety in our datasets in terms of the fraction of triangles that are open, the average degree, and the edge density. Local statistics at the level of egonets can identify system domain, which suggests that these features are key to the organizing principles of the systems. Recent research shows the small fraction of triangles that are open in coauthorship networks [51]; our results are consistent but reveal that open triangles are extremely common in other domains. Prior research has also identified the distinction between open and closed triangles when projecting bipartite networks but have not studied the idea of simplicial closure events [44, 45].

We found that common principles from dyadic network evolution also hold for higher-order structure, namely, tie strength and edge density are positive indicators of simplicial closure events amongst sets of three and four nodes. However, there is tension between these features—the more influential feature depends on the dataset, suggesting different mechanisms for simplicial closure events. For example, edge density matters more in human interaction, but tie strength matters more for tagging on online discussion platforms.

Higher-order link prediction provides a general methodology for evaluating models in any data where higher-order structure

evolves over time, such as predicting which sets of authors will write a paper together or which sets of people will appear as joint recipients on an email. We anticipate that higher-order link prediction will validate emerging higher-order network modeling techniques, such as multipartite networks [35], meta paths [62], embeddings [21], and connect to ideas in computational topology, such as random walks on simplicial complexes [40, 50]. Related higher-order models for different data [56, 67] can also use higher-order link prediction for model evaluation. For example, in the absence of temporal information, higher-order link prediction could be used to find missing data, similar to how dyadic link prediction can find missing data in static networks [12]. Our higher-order link prediction framework also provides a way to study more sophisticated models where the underlying network is also dynamic, e.g., with arrival and departure of nodes. Specifically, such models should be able to predict higher-order links.

Our prediction problem examined a structure that is not even considered in traditional network analysis, where no distinction is made between open and closed triangles. From this setup, we found that simple local measures (generalized means of edge weights) are effective predictors. This finding differs from traditional link prediction, where long paths are important [34] and suggests that the temporal evolution of higher-order network data is fundamentally different than dyadic network evolution.

Data and software availability. All datasets except the Congress and music ones are available at <http://www.cs.cornell.edu/~arb/data/>. Software is available at <https://github.com/arbenson/SchOLP-Tutorial>.

Acknowledgements

We thank Mason Porter and Peter Mucha for providing the Congress committees dataset. We thank Paul Horn, Gabor Lippner, and Jarosław Błasiok for helpful discussion. This research was supported in part by a Simons Investigator Award. ARB was supported in part by NSF Award DMS-1830274. RA was supported in part by a Google scholarship and a Facebook scholarship. AJ received funding from the Vannevar Bush Fellowship from the office of the Secretary of Defense. MTS received funding from the European Union’s Horizon 2020 research and innovation programme under the Marie Skłodowska-Curie grant agreement No 702410.

REFERENCES

- [1] Lada A Adamic and Eytan Adar. 2003. Friends and neighbors on the web. *Social networks* 25, 3 (2003), 211–230.
- [2] Réka Albert and Albert-László Barabási. 2002. Statistical mechanics of complex networks. *Reviews of Modern Physics* 74, 1 (jan 2002), 47–97. <https://doi.org/10.1103/revmodphys.74.47>
- [3] Lars Backstrom, Dan Huttenlocher, Jon Kleinberg, and Xiangyang Lan. 2006. Group formation in large social networks: membership, growth, and evolution. In *Proceedings of the 12th ACM SIGKDD international conference on Knowledge discovery and data mining*. ACM, 44–54.
- [4] Lars Backstrom and Jure Leskovec. 2011. Supervised Random Walks: Predicting and Recommending Links in Social Networks. In *Proceedings of the Fourth ACM International Conference on Web Search and Data Mining (WSDM '11)*. ACM, New York, NY, USA, 635–644. <https://doi.org/10.1145/1935826.1935914>
- [5] Bahman Bahmani, Abdur Chowdhury, and Ashish Goel. 2010. Fast incremental and personalized PageRank. *Proceedings of the VLDB Endowment* 4, 3 (2010), 173–184.
- [6] Grey Ballard, Tamara G Kolda, Ali Pinar, and C Seshadhri. 2015. Diamond sampling for approximate maximum all-pairs dot-product (MAD) search. In *IEEE International Conference on Data Mining*. IEEE, 11–20.

- [7] A.L. Barabási, H. Jeong, Z. Néda, E. Ravasz, A. Schubert, and T. Vicsek. 2002. Evolution of the social network of scientific collaborations. *Physica A: Statistical Mechanics and its Applications* 311, 3-4 (aug 2002), 590–614. [https://doi.org/10.1016/s0378-4371\(02\)00736-7](https://doi.org/10.1016/s0378-4371(02)00736-7)
- [8] A. R. Benson, D. F. Gleich, and J. Leskovec. 2016. Higher-order organization of complex networks. *Science* 353, 6295 (jul 2016), 163–166. <https://doi.org/10.1126/science.aad9029>
- [9] Claude Berge. 1989. *Hypergraphs*. Elsevier.
- [10] Ed Bullmore and Olaf Sporns. 2009. Complex brain networks: graph theoretical analysis of structural and functional systems. *Nature Reviews Neuroscience* 10, 3 (2009), 186.
- [11] Norishige Chiba and Takao Nishizeki. 1985. Arboricity and subgraph listing algorithms. *SIAM J. Comput.* 14, 1 (1985), 210–223.
- [12] Aaron Clauset, Cristopher Moore, and M. E. J. Newman. 2008. Hierarchical structure and the prediction of missing links in networks. *Nature* 453, 7191 (may 2008), 98–101. <https://doi.org/10.1038/nature06830>
- [13] Jesse Davis and Mark Goadrich. 2006. The relationship between Precision-Recall and ROC curves. In *Proceedings of the 23rd International Conference on Machine Learning*. 233–240.
- [14] Charlotte M. Deane, Łukasz Salwiński, Ioannis Xenarios, and David Eisenberg. 2002. Protein Interactions: two methods for assessment of the reliability of high throughput observations. *Molecular & Cellular Proteomics* 1, 5 (apr 2002), 349–356. <https://doi.org/10.1074/mcp.m100037-mcp200>
- [15] David Easley and Jon Kleinberg. 2010. *Networks, crowds, and markets: Reasoning about a highly connected world*. Cambridge University Press.
- [16] Scott L. Feld. 1981. The focused organization of social ties. *Amer. J. Sociology* 86, 5 (1981).
- [17] James H. Fowler. 2006. Connecting the Congress: A Study of Cosponsorship Networks. *Political Analysis* 14, 04 (2006), 456–487. <https://doi.org/10.1093/pan/mp1002>
- [18] James H. Fowler. 2006. Legislative cosponsorship networks in the US House and Senate. *Social Networks* 28, 4 (oct 2006), 454–465. <https://doi.org/10.1016/j.socnet.2005.11.003>
- [19] Peter Frankl. 1995. Extremal set systems. In *Handbook of combinatorics*, Ron Graham, Martin Grötschel, and Laszlo Lovasz (Eds.). Vol. 1. Elsevier.
- [20] Amir Ghasemian, Homa Hosseinmardi, and Aaron Clauset. 2018. Evaluating overfit and underfit in models of network community structure. *arXiv:1802.10582* (2018).
- [21] Palash Goyal and Emilio Ferrara. 2017. Graph embedding techniques, applications, and performance: A survey. *arXiv preprint 1705.02801* (2017).
- [22] Mark S Granovetter. 1973. The strength of weak ties. *Amer. J. Sociology* 78, 6 (1973), 1360–1380.
- [23] Jacopo Grilli, György Barabás, Matthew J. Michalska-Smith, and Stefano Allesina. 2017. Higher-order interactions stabilize dynamics in competitive network models. *Nature* (jul 2017). <https://doi.org/10.1038/nature23273>
- [24] Aditya Grover and Jure Leskovec. 2016. node2vec: Scalable Feature Learning for Networks. In *Proceedings of the 22nd ACM SIGKDD International Conference on Knowledge Discovery and Data Mining*. ACM Press. <https://doi.org/10.1145/2939672.2939754>
- [25] Allen Hatcher. 2002. *Algebraic topology*. Cambridge University Press.
- [26] Willem J Heiser and Mohammed Bannani. 1997. Triadic distance models: axiomatization and least squares representation. *Journal of Mathematical Psychology* 41, 2 (1997), 189–206.
- [27] Leo Katz. 1953. A new status index derived from sociometric analysis. *Psychometrika* 18, 1 (1953), 39–43.
- [28] Tatsuhiro Kawamoto and Yoshiyuki Kabashima. 2017. Cross-validation estimate of the number of clusters in a network. *Scientific Reports* 7, 1 (jun 2017). <https://doi.org/10.1038/s41598-017-03623-x>
- [29] M. Kivela, A. Arenas, M. Barthelemy, J. P. Gleeson, Y. Moreno, and M. A. Porter. 2014. Multilayer networks. *Journal of Complex Networks* 2, 3 (jul 2014), 203–271. <https://doi.org/10.1093/comnet/cnu016>
- [30] Bryan Klimt and Yiming Yang. 2004. Introducing the Enron Corpus. In *CEAS*.
- [31] Gueorgi Kossinets and Duncan J Watts. 2006. Empirical analysis of an evolving social network. *Science* 311, 5757 (2006), 88–90.
- [32] Matthieu Latapy. 2008. Main-memory triangle computations for very large (sparse (power-law)) graphs. *Theoretical Computer Science* 407, 1-3 (2008), 458–473.
- [33] Jure Leskovec, Lars Backstrom, Ravi Kumar, and Andrew Tomkins. 2008. Microscopic evolution of social networks. In *Proceeding of the 14th ACM SIGKDD international conference on Knowledge discovery and data mining*. ACM Press. <https://doi.org/10.1145/1401890.1401948>
- [34] David Liben-Nowell and Jon Kleinberg. 2007. The link-prediction problem for social networks. *Journal of the American Society for Information Science and Technology* 58, 7 (2007), 1019–1031. <https://doi.org/10.1002/asi.20591>
- [35] P G Lind and H J Herrmann. 2007. New approaches to model and study social networks. *New Journal of Physics* 9, 7 (2007).
- [36] Linyuan Lü and Tao Zhou. 2011. Link prediction in complex networks: A survey. *Physica A: Statistical Mechanics and its Applications* 390, 6 (mar 2011), 1150–1170. <https://doi.org/10.1016/j.physa.2010.11.027>
- [37] Rossana Mastrandrea, Julie Fournet, and Alain Barrat. 2015. Contact patterns in a high school: a comparison between data collected using wearable sensors, contact diaries and friendship surveys. *PLoS one* 10, 9 (2015), e0136497.
- [38] Changping Meng, S Chandra Mouli, Bruno Ribeiro, and Jennifer Neville. 2018. Subgraph Pattern Neural Networks for High-Order Graph Evolution Prediction. In *Proceedings of the AAAI Conference on Artificial Intelligence*.
- [39] R. Milo. 2002. Network Motifs: Simple Building Blocks of Complex Networks. *Science* 298, 5594 (oct 2002), 824–827. <https://doi.org/10.1126/science.298.5594.824>
- [40] Sayan Mukherjee and John Steenbergen. 2016. Random walks on simplicial complexes and harmonics. *Random Structures & Algorithms* 49, 2 (mar 2016), 379–405. <https://doi.org/10.1002/rsa.20645>
- [41] Saket Navlakha and Carl Kingsford. 2010. The power of protein interaction networks for associating genes with diseases. *Bioinformatics* 26, 8 (2010), 1057–1063.
- [42] Mark EJ Newman. 2001. Clustering and preferential attachment in growing networks. *Physical review E* 64, 2 (2001), 025102.
- [43] M. E. J. Newman. 2003. The Structure and Function of Complex Networks. *SIAM Rev.* 45, 2 (jan 2003), 167–256. <https://doi.org/10.1137/s003614450342480>
- [44] M. E. J. Newman, Duncan J. Watts, and Steven H. Strogatz. 2002. Random graph models of social networks. *Proceedings of the National Academy of Sciences* 99, Suppl1 (2002).
- [45] Tore Opsahl. 2013. Triadic closure in two-mode networks: Redefining the global and local clustering coefficients. *Social Networks* 35, 2 (may 2013), 159–167. <https://doi.org/10.1016/j.socnet.2011.07.001>
- [46] Lawrence Page, Sergey Brin, Rajeev Motwani, and Terry Winograd. 1999. *The PageRank Citation Ranking: Bringing Order to the Web*. Technical Report 1999-66. Stanford University. <http://dbpubs.stanford.edu:8090/pub/1999-66>
- [47] C. C. Paige and M. A. Saunders. 1975. Solution of Sparse Indefinite Systems of Linear Equations. *SIAM J. Numer. Anal.* 12, 4 (1975), 617–629. <https://doi.org/10.1137/0712047>
- [48] Christopher C. Paige and Michael A. Saunders. 1982. LSQR: An Algorithm for Sparse Linear Equations and Sparse Least Squares. *ACM Trans. Math. Software* 8, 1 (mar 1982), 43–71. <https://doi.org/10.1145/355984.355989>
- [49] Ashwin Paranjape, Austin R Benson, and Jure Leskovec. 2017. Motifs in temporal networks. In *Proceedings of the Tenth ACM International Conference on Web Search and Data Mining*. ACM, 601–610.
- [50] Ori Parzanchevski and Ron Rosenthal. 2016. Simplicial complexes: Spectrum, homology and random walks. *Random Structures & Algorithms* 50, 2 (may 2016), 225–261. <https://doi.org/10.1002/rsa.20657>
- [51] Alice Patania, Giovanni Petri, and Francesco Vaccarino. 2017. The shape of collaborations. *EPJ Data Science* 6, 1 (aug 2017). <https://doi.org/10.1140/epjds/s13688-017-0114-8>
- [52] F. Pedregosa, G. Varoquaux, A. Gramfort, V. Michel, B. Thirion, O. Grisel, M. Blondel, P. Prettenhofer, R. Weiss, V. Dubourg, J. Vanderplas, A. Passos, D. Cournapeau, M. Brucher, M. Perrot, and E. Duchesnay. 2011. Scikit-learn: Machine Learning in Python. *Journal of Machine Learning Research* 12 (2011), 2825–2830.
- [53] Ali Pinar, C. Seshadhri, and Vaidyanathan Vishal. 2017. ESCAPE: Efficiently Counting All 5-Vertex Subgraphs. In *Proceedings of the 26th International Conference on World Wide Web (WWW '17)*. International World Wide Web Conferences Steering Committee, Republic and Canton of Geneva, Switzerland, 1431–1440. <https://doi.org/10.1145/3038912.3052597>
- [54] Mason A. Porter, Peter J. Mucha, M.E.J. Newman, and A.J. Friend. 2007. Community structure in the United States House of Representatives. *Physica A: Statistical Mechanics and its Applications* 386, 1 (dec 2007), 414–438. <https://doi.org/10.1016/j.physa.2007.07.039>
- [55] M. A. Porter, P. J. Mucha, M. E. J. Newman, and C. M. Warmbrand. 2005. A network analysis of committees in the U.S. House of Representatives. *Proceedings of the National Academy of Sciences* 102, 20 (may 2005), 7057–7062. <https://doi.org/10.1073/pnas.0500191102>
- [56] Martin Rosvall, Alcides V. Esquivel, Andrea Lancichinetti, Jevin D. West, and Renaud Lambiotte. 2014. Memory in network flows and its effects on spreading dynamics and community detection. *Nature Communications* 5, 1 (aug 2014). <https://doi.org/10.1038/ncomms5630>
- [57] Marc Santolini and Albert-László Barabási. 2018. Predicting perturbation patterns from the topology of biological networks. *Proceedings of the National Academy of Sciences* 115, 27 (jun 2018), E6375–E6383. <https://doi.org/10.1073/pnas.1720589115>
- [58] Michael T Schaub, Austin R Benson, Paul Horn, Gabor Lippner, and Ali Jadbabaie. 2018. Random Walks on Simplicial Complexes and the normalized Hodge Laplacian. *arXiv preprint arXiv:1807.05044* (2018).
- [59] Aneesh Sharma, C Seshadhri, and Ashish Goel. 2017. When Hashes Met Wedges: A Distributed Algorithm for Finding High Similarity Vectors. In *Proceedings of the 26th International Conference on World Wide Web*. International World Wide Web Conferences Steering Committee, 431–440.
- [60] Arnab Sinha, Zhihong Shen, Yang Song, Hao Ma, Darrin Eide, Bo-june Paul Hsu, and Kuansan Wang. 2015. An overview of Microsoft Academic Service (MAS)

- and applications. In *Proceedings of the 24th international conference on world wide web*. ACM, 243–246.
- [61] Juliette Stehlé, Nicolas Voirin, Alain Barrat, Ciro Cattuto, Lorenzo Isella, Jean-François Pinton, Marco Quaggiotto, Wouter Van den Broeck, Corinne Régis, Bruno Lina, et al. 2011. High-resolution measurements of face-to-face contact patterns in a primary school. *PLoS one* 6, 8 (2011), e23176.
- [62] Yizhou Sun, Jiawei Han, Charu C. Aggarwal, and Nitesh V. Chawla. 2012. When will it happen?: relationship prediction in heterogeneous information networks. In *Proceedings of the fifth ACM international conference on Web search and data mining*. ACM Press. <https://doi.org/10.1145/2124295.2124373>
- [63] Jie Tang, Sen Wu, Jimeng Sun, and Hang Su. 2012. Cross-domain collaboration recommendation. In *Proceedings of the 18th ACM SIGKDD international conference on Knowledge discovery and data mining*. ACM Press. <https://doi.org/10.1145/2339530.2339730>
- [64] J. Ugander, L. Backstrom, C. Marlow, and J. Kleinberg. 2012. Structural diversity in social contagion. *Proceedings of the National Academy of Sciences* 109, 16 (apr 2012), 5962–5966. <https://doi.org/10.1073/pnas.1116502109>
- [65] Chao Wang, Venu Satuluri, and Srinivasan Parthasarathy. 2007. Local probabilistic models for link prediction. In *Seventh IEEE International Conference on Data Mining*. IEEE, 322–331.
- [66] X. Wang, N. Gulbahce, and H. Yu. 2011. Network-based methods for human disease gene prediction. *Briefings in Functional Genomics* 10, 5 (jul 2011), 280–293. <https://doi.org/10.1093/bfgp/elr024>
- [67] Jian Xu, Thanuka L. Wickramaratne, and Nitesh V. Chawla. 2016. Representing higher-order dependencies in networks. *Science Advances* 2, 5 (may 2016), e1600028. <https://doi.org/10.1126/sciadv.1600028>

A DATASET COLLECTION AND CONSTRUCTION

Here we provide a more complete description of the datasets.

Coauthorship. In these datasets, the nodes correspond to authors, and each simplex represents the authors on a scientific publication. The timestamp is the year of publication. We analyze three coauthorship networks—one derived from DBLP, an online bibliography for computer science, and two derived from the Microsoft Academic Graph (MAG). We used the September 3, 2017 release of DBLP³ and the MAG version released with the Open Academic Graph⁴ [60]. We constructed two field-specific datasets by filtering the MAG data according to keywords in the “field of study” information. One dataset consisted of all papers with “History” as a field of study and the other all papers with “Geology” as a field of study.

Stack Exchange tags. Stack Exchange is a collection of question-and-answer web sites.⁵ Users post questions and may annotate each question with up to 5 tags that specify topic areas spanned by the question. We derive tag networks where nodes correspond to tags and each simplex represents the tags on a question. The timestamp for a simplex is the time that the question was posted on the web site. We derived three datasets corresponding to three stack exchange web sites: Stack Overflow,⁶ Mathematics Stack Exchange,⁷ and Ask Ubuntu.⁸ The raw data was downloaded from the Stack Exchange data dump,⁹ which contains the complete history of the content on the stack exchange web sites.

Stack Exchange threads. We also formed user interaction datasets from the stack exchange web sites. Users post answers to questions, creating a question-and-answer “thread.” The nodes are users and simplices correspond to the users asking a question or posting an answer on a single thread. We only considered threads where the question and all answers were posted within 24 hours. The timestamps of the simplices are the times that the question was posted.

National Drug Code Directory (NDC). Under the Drug Listing Act of 1972, the U.S. Food and Drug Administration releases information on all commercial drugs going through the regulation of the agency. We constructed two datasets from this data where simplices correspond to drugs. In one, the nodes are classification labels (e.g., serotonin reuptake inhibitor), and simplices are comprised of all labels applied to a drug; in the other, the nodes are substances (e.g., testosterone) and simplices are constructed from all substances in a drug. In both derived datasets, the timestamps are the days when the drugs were first marketed.

United States Congress. We derived two datasets from political networks, where the nodes are congresspersons in the U.S. congress. In the first, simplices represent all members of committees and sub-committees in the House of Representatives (Congresses 101 to 107, from 1989 to 2003), and the timestamp of the simplex is the year that the committee formed [54, 55]. In the second dataset,

simplices are comprised of the sponsor and co-sponsors of legislative bills put forth in the House of Representatives and the Senate [17, 18], and the timestamps are the days that the bills were introduced.

Email. In email communication, messages can be sent to multiple recipients. We analyze two email datasets—one from communication between Enron employees [30] and the other from a European research institution [49]. In both datasets, nodes are email addresses. In the Enron dataset, a simplex consists of the sender and all recipients of an email. The data source for the European research institution only contains (sender, receiver, timestamp) tuples, where timestamps are recorded at 1-second resolution [49]. Simplices consist of a sender and all receivers such that the email between the two has the same timestamp.

Human contact. The human contact networks are constructed from interactions recorded by wearable sensors in a high school [37] and a primary school [61]. The sensors record proximity-based contacts every 20 seconds. We construct a graph for each interval, where nodes i and j are connected if they are in contact during the interval. Simplices are all maximal cliques in the graph at each time interval.

DAWN. The Drug Abuse Warning Network (DAWN) is a national health surveillance system that records drug use contributing to hospital emergency department visits throughout the United States. Simplices in our dataset are the drugs used by a patient (as reported by the patient) in an emergency department visit. The drugs include illicit substances, prescription and over-the-counter medication, and dietary supplements. Timestamps of visits are recorded at the resolution of quarter-years, spanning a total duration of 8 years. For a period of time, the recording system only recorded the first 16 drugs reported by a patient, so we only use (at most) the first 16 drugs reported by a patient for the entire dataset.

Music collaboration. Musical artists often collaborate on individual songs. We derive a dataset where nodes are artists and a simplex consists of all artists collaborating on a song. The songs were obtained from a web crawl of the music lyrics web site Genius.¹⁰ We consider the collaborating artists to be the lead artist along with any “featured” artists (this excludes some cases where lyrics from an artist are included but that artist is not listed as a featured artist). The timestamps are the release dates of the songs. We only collected data from songs that contain the “rap” tag on the web site and discarded songs without a specified release date. The crawler ran for several days and collected over 500,000 songs.

³<http://dblp.org/xml/release/>

⁴<https://www.openacademic.ai/oag/>

⁵<https://stackexchange.com>

⁶<https://stackoverflow.com>

⁷<https://math.stackexchange.com>

⁸<https://askubuntu.com>

⁹<https://archive.org/details/stackexchange>; downloaded September 20, 2017.

¹⁰<https://genius.com/>

B TEMPORAL ASYNCHRONY AND OPEN TRIANGLES

Our datasets contain temporal dynamics, so edges may only be “active” for certain periods in the total time spanned by the dataset. This provides one plausible explanation for the existence of open triangles. For example, in coauthorship networks, an open triangle may arise when three separate collaborations occurred in disjoint time periods. To investigate the importance of such effects, we analyze the temporal asynchrony in open triangles in our datasets. Let the “active interval” of an edge in the projected graph be the interval bounded by the earliest and latest timestamps of simplices containing the two nodes in the edge. Recall that our datasets are defined by a collection of timestamped simplices $\{(S_i, t_i)\}$, where each $S_i \subset V$ is the simplex and each $t_i \in \mathbb{R}$ is a timestamp. The active interval of an edge (u, v) is then

$$I_{u,v} = [\min\{t_i \mid u, v \in S_i\}, \max\{t_i \mid u, v \in S_i\}]. \quad (3)$$

For each open triangle in each dataset, we compute the number of pairwise overlapping active intervals amongst the three edges in the triangle (Table 4). In the majority of cases, all three pairs of intervals overlap. By Helly’s theorem, there is an interval of time for which all three edges in the open triangle are simultaneously active. Stated differently, in the coauthorship example, the collaborators could have theoretically formed a closed triangle during this time period, but they did not. We conclude that temporal asynchrony is not a major reason for the presence of open triangles in our datasets.

Table 4: Temporal asynchrony and open triangles. For each open triangle in each dataset, we find the number of overlaps between the active intervals of the three edges, where an active interval of an edge has end points given by the earliest and latest timestamps of simplices containing the two nodes in the edge (Eq. (3)). The edges in most open triangles have three pairwise overlapping intervals. In these cases, there is a time period where all three edges were simultaneously active by Helly’s theorem.

Dataset	# open triangles	# overlaps			
		0	1	2	3
coauth-DBLP	1,295,214	0.012	0.143	0.123	0.722
coauth-MAG-history	96,420	0.002	0.055	0.059	0.884
coauth-MAG-geology	2,494,960	0.010	0.128	0.109	0.753
tags-stack-overflow	300,646,440	0.002	0.067	0.071	0.860
tags-math-sx	2,666,353	0.001	0.040	0.049	0.910
tags-ask-ubuntu	3,288,058	0.002	0.088	0.085	0.825
threads-stack-overflow	99,027,304	0.001	0.034	0.037	0.929
threads-math-sx	11,294,665	0.001	0.038	0.039	0.922
threads-ask-ubuntu	136,374	0.000	0.020	0.023	0.957
NDC-substances	1,136,357	0.020	0.196	0.151	0.633
NDC-classes	9,064	0.022	0.191	0.136	0.652
DAWN	5,682,552	0.027	0.216	0.155	0.602
congress-committees	190,054	0.001	0.046	0.058	0.895
congress-bills	44,857,465	0.003	0.063	0.113	0.821
email-Enron	3,317	0.008	0.130	0.151	0.711
email-Eu	234,600	0.010	0.131	0.132	0.727
contact-high-school	31,850	0.000	0.015	0.019	0.966
contact-primary-school	98,621	0.000	0.012	0.014	0.974
music-rap-genius	70,057	0.028	0.221	0.141	0.611

C SIMPLICIAL CLOSURE PROBABILITIES

We now present simplicial closure event probabilities on three and four nodes. The setup is the same as in Section 3. We split the data into training and test sets, corresponding to the first 80% and final 20% of time-ordered simplices, respectively. Given the configuration of a set of three or four nodes in the training data, we measure the probability that the nodes go through a simplicial closure event in the final 20% of the data.

In the case of 3-node simplicial closure events, we determine the open configuration in the training set by examining the three nodes in the projected graph. Effectively, we examined how many times each of the three *2-node subsets* co-appeared in a simplex. Figure 8 shows a heat map of the closure probabilities as a function of the open 3-node configuration.

For 4-node open configurations we proceed analogously, using the corresponding *3-node subsets*. Specifically, for a given set of 4 nodes, every triangle in the projected graph is classified as either (i) an open simplicial tie, i.e., the triangle is open; (ii) a weak simplicial tie, meaning that the three nodes have appeared in just one simplex together; or (iii) a strong simplicial tie, meaning that the three nodes have appeared in at least two simplices together. In contrast to the 3-node case, these 4-node configurations are not completely determined by the weighted projected graph, since the projected graph (as defined) does not contain information on whether or not 3 nodes induce a closed triangle. Thus, with 4-node simplices, we make use of additional topological information provided in our set-valued datasets.

One could also account for the tie strengths of the 2-node subsets (edges) in a 4-node configuration—a complete characterization of the possible induced configurations leading to a simplicial closure event is much more complex for the 4-node case than the 3-node case. For an accessible study on the closure patterns of 4-node simplices, we measure the probability of closure with respect to the 27 open configurations where the induced 4-node subgraph in the projected graph contains at least one triangle. Our classification distinguishes triangles by tie strength (open, weak, or closed), but not by edge tie strengths, other than by what is implied by the triangles. Figure 9 shows a heat map of the closure probabilities as a function of the open 4-node configuration.

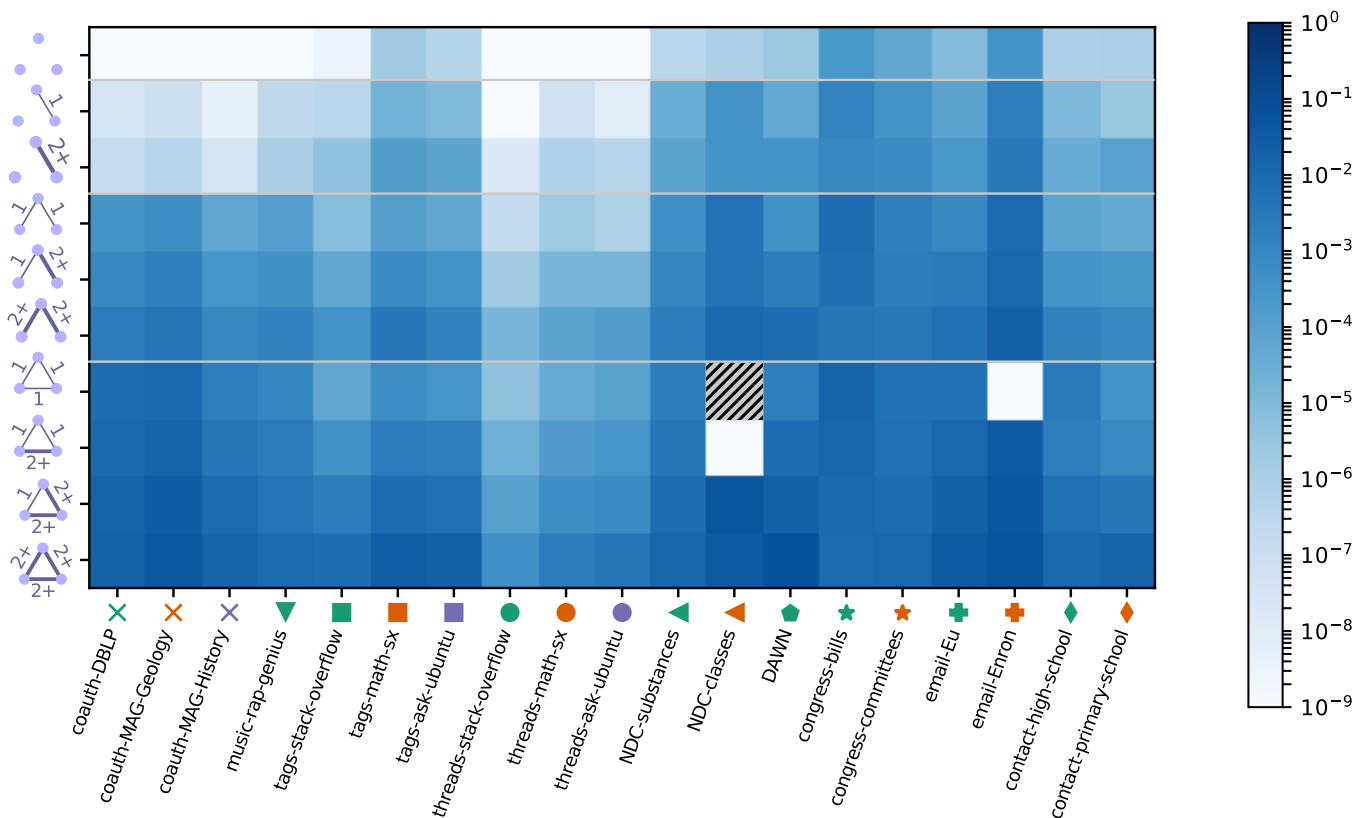


Figure 8: Heat map of the probabilities of simplicial closure events as a function of the 3-node open configuration. We use the first 80% of the timestamped data to determine the configuration of every 3-node set and compute the probability that the set appears in a simplex in the final 20% of the data, conditioned on the open configuration. Shaded boxes are configurations that appear 20 or fewer times in the first 80% of the data. The four sections of the heat map correspond to 0, 1, 2, or 3 edges in the induced subgraph.

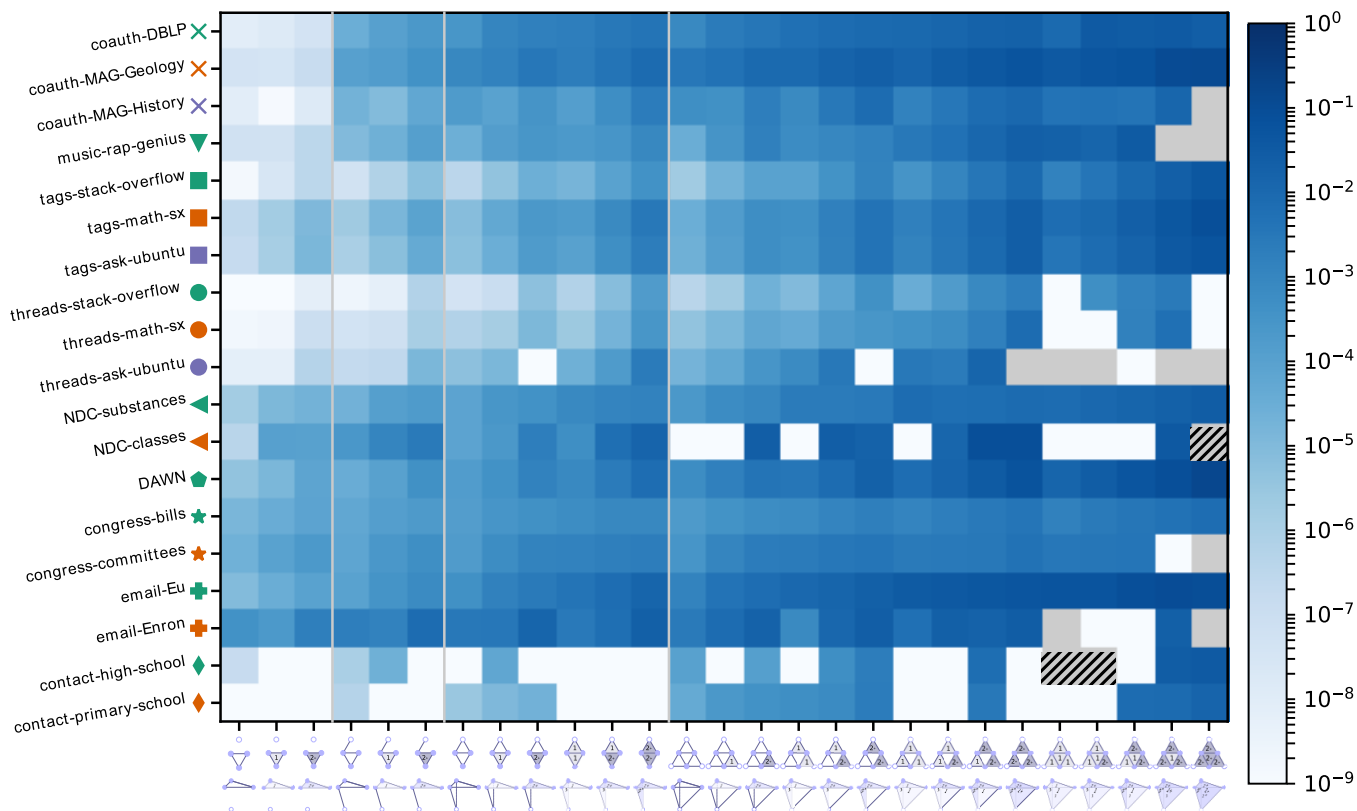


Figure 9: Heat map of the probabilities of simplicial closure events as a function of the 4-node open configuration. We use the first 80% of the timestamped data to determine the configuration of every 4-node set that contains at least 1 triangle and does not appear in a simplex. We then compute the probability that a 4-node set appears in a simplex in the final 20% of the data, conditioned on the open configuration. In an open configuration, there are three types of simplicial tie strengths for a triangle—open, weak, and strong—given by the number of times the three nodes in the triangle have co-appeared in a simplex (zero, one, or at least two times). Shaded boxes are configurations that appear 20 or fewer times in the first 80% of the data. We illustrate each subgraph configuration on the x-axis with a projection of the simplex onto two dimensions (top line—the unfilled circle represents the same node) as well as a tetrahedral three-dimensional perspective figure (bottom line). The four sections of the heat map correspond to 3, 4, 5, or 6 edges in the configuration.

D SIMPLICIAL CLOSURE EVENTS AT DIFFERENT POINTS IN TIME

In Section 3, we studied simplicial closure events by counting the 3-node and 4-node configuration patterns in the first 80% of timestamped simplices and then measuring the fraction of instances that experience a simplicial close event in the final 20% of timestamped simplices. Here, we show that our results are consistent when examining different time slices of the data. We first filtered each dataset to contain only the first $X\%$ of timestamped simplices, for $X = 40, 60, 80$ (the original dataset is the case of $X = 100$.) We then split the filtered dataset into the first 80% and last 20% of timestamped simplices (within the time frame of the filtered dataset) and computed the probabilities of simplicial closure events.







Table 6 lists the 3-node simplicial closure event probabilities as a function of the configuration of the 3 nodes in the first 80% of the data for $X = 40, 60, 80, 100$, and Figure 10 provides the heat maps for each value of X (analogous to the heat map in Figure 8). Broadly, the closure probabilities remain similar for different values of X . We also find that edge density and tie strength are always positive indicators of simplicial closure events, regardless of X (Table 5). Thus, these features are important for simplicial closure events throughout the history of the network dynamics.





The tension between these features is also consistent over time. The weak open triangle (where all three edges are weak ties) is more likely to close than the strong wedge (the 3-node configuration with exactly two strong ties) in the coauth-DBLP, coauth-MAG-Geology, and congress-bills datasets for all values of X as well as in the congress-committees dataset for $X = 60, 80, 100$. On the other hand, the strong wedge is more likely to close in the three stack exchange tags networks, DAWN, and threads-stack-overflow for all values of X as well as in threads-math-sx for $X = 80, 100$.

Table 5: Consistency in the effects of tie strength and edge density in 3-node configurations on simplicial closure events at different points in time. For edge density, we tested whether or not the closure event probability of a fixed weighted induced subgraph configuration and the same configuration with an additional unit-weight edge significantly increases or decreases the closure probability (at significance level 10^{-5}). For tie strength, we tested whether the closure event probability significantly increases or decreases when comparing a fixed weighted induced subgraph containing at least one weak tie, and the same configuration where the weak tie is converted to a strong tie (edge weight at least 2 in the projected graph). The “total” column is the number of tested hypotheses. We apply the tests to filtered datasets that only contain the first $X\%$ of timestamped simplices (in time order). We only consider cases where the configuration has at least 25 samples in the first 80% of timestamped simplices of a filtered dataset. Increasing either edge density or tie strength significantly increases the closure probability for all values of X , suggesting that these features are positive indicators of simplicial closure over time.

X	edge density increases			tie strength increases		
	sig. incr.	sig. decr.	total	sig. incr.	sig. decr.	total
40	89	0	113	71	2	113
60	101	0	113	80	7	113
80	102	0	113	86	2	113
100	96	0	107	76	6	107

Table 6: Simplicial closure event probabilities of different configurations at different points in time. We first filtered each dataset to contain only the first $X\%$ of timestamped simplices, for $X = 40, 60, 80, 100$. We then split the filtered dataset into the first 80% and last 20% of timestamped simplices (within the time frame of the filtered dataset). We record the probability of closure in last 20% conditioned on the open configuration in the first 80%.

																								
	40	60	80	100	40	60	80	100	40	60	80	100	40	60	80	100	40	60	80	100	40	60	80	100
coauth-DBLP	8.2e-13	1.2e-12	8.3e-13	9.3e-13	3.1e-08	4.2e-08	3.4e-08	3.6e-08	1.1e-07	1.5e-07	1.2e-07	1.3e-07	4.4e-04	5.2e-04	3.8e-04	3.5e-04	9.7e-04	1.2e-03	9.4e-04	8.8e-04	2.0e-03	2.5e-03	2.2e-03	2.1e-03
coauth-MAG-Geology	7.9e-12	5.0e-12	3.2e-12	4.2e-12	1.1e-07	9.9e-08	7.6e-08	8.9e-08	4.1e-07	4.6e-07	3.6e-07	4.5e-07	5.8e-04	6.8e-04	5.1e-04	5.3e-04	1.4e-03	1.8e-03	1.5e-03	1.6e-03	3.0e-03	4.4e-03	3.7e-03	4.1e-03
coauth-MAG-History	1.2e-12	8.8e-13	3.3e-13	1.8e-13	2.7e-08	2.0e-08	1.0e-08	5.6e-09	1.6e-07	1.4e-07	6.3e-08	3.9e-08	1.4e-04	1.8e-04	1.0e-04	6.3e-05	6.2e-04	8.5e-04	4.1e-04	2.9e-04	1.3e-03	2.3e-03	2.5e-03	1.0e-03
music-rap-genius	1.6e-09	8.6e-10	4.3e-10	1.2e-10	1.3e-06	6.2e-07	5.7e-07	2.3e-07	5.5e-06	2.9e-06	1.9e-06	1.1e-06	3.3e-04	2.2e-04	2.2e-04	1.3e-04	1.0e-03	8.0e-04	5.6e-04	4.4e-04	3.3e-03	2.9e-03	1.7e-03	1.3e-03
tags-stack-overflow	3.6e-09	3.5e-09	2.9e-09	2.8e-09	4.8e-07	4.5e-07	3.8e-07	3.8e-07	5.0e-06	4.6e-06	4.2e-06	4.2e-06	9.6e-06	8.5e-06	7.4e-06	7.4e-06	6.9e-05	6.3e-05	5.8e-05	5.7e-05	4.6e-04	4.1e-04	3.8e-04	3.7e-04
tags-math-sx	1.0e-06	1.4e-06	1.9e-06	1.9e-06	1.7e-05	1.7e-05	1.9e-05	2.1e-05	1.1e-04	1.1e-04	1.5e-04	1.4e-04	1.3e-04	1.2e-04	1.3e-04	1.2e-04	7.0e-04	7.0e-04	7.2e-04	6.9e-04	3.4e-03	3.3e-03	3.4e-03	3.2e-03
tags-ask-ubuntu	4.9e-07	5.4e-07	7.9e-07	4.8e-07	1.1e-05	1.3e-05	1.4e-05	9.8e-06	8.1e-05	9.7e-05	1.1e-04	7.9e-05	9.4e-05	8.8e-05	8.6e-05	6.2e-05	4.8e-04	4.6e-04	4.7e-04	3.8e-04	1.5e-03	1.6e-03	1.5e-03	1.4e-03
threads-stack-overflow	3.2e-12	8.4e-13	4.3e-13	2.2e-13	5.5e-09	2.2e-09	1.4e-09	9.0e-10	8.4e-08	4.2e-08	2.7e-08	2.1e-08	6.4e-07	3.3e-07	2.5e-07	1.9e-07	4.8e-06	3.0e-06	2.3e-06	2.0e-06	2.5e-05	1.7e-05	1.5e-05	1.5e-05
threads-math-sx	2.3e-10	1.4e-10	6.4e-11	4.2e-11	1.5e-07	1.3e-07	7.8e-08	6.0e-08	1.2e-06	1.3e-06	9.4e-07	7.4e-07	3.6e-06	3.8e-06	2.5e-06	2.3e-06	1.6e-05	2.0e-05	1.7e-05	1.5e-05	6.4e-05	8.9e-05	9.0e-05	7.9e-05
threads-ask-ubuntu	5.3e-11	1.4e-11	5.3e-12	3.2e-12	2.8e-08	2.1e-08	1.2e-08	9.0e-09	5.7e-07	5.2e-07	5.7e-07	4.1e-07	1.7e-06	5.6e-07	7.7e-07	7.8e-07	1.6e-05	1.4e-05	1.8e-05	1.6e-05	6.8e-05	1.0e-04	1.6e-04	1.4e-04
NDC-substances	1.4e-06	3.4e-06	9.6e-07	3.8e-07	1.1e-04	1.9e-04	7.5e-05	3.3e-05	1.9e-04	4.2e-04	1.9e-04	7.8e-05	2.5e-03	2.9e-03	1.4e-03	4.8e-04	6.0e-03	6.0e-03	3.2e-03	1.1e-03	1.0e-02	1.2e-02	6.7e-03	2.2e-03
NDC-classes	5.3e-07	9.0e-06	1.5e-06	8.4e-07	3.7e-06	8.8e-04	1.7e-04	3.1e-04	3.6e-04	1.8e-03	7.7e-04	3.4e-04	0.0e+00	4.0e-02	0.0e+00	4.8e-03	0.0e+00	7.1e-02	3.0e-03	4.8e-03	9.1e-03	5.4e-02	2.4e-02	1.1e-02
DAWN	1.5e-06	2.1e-06	2.7e-06	2.5e-06	4.2e-05	4.6e-05	6.0e-05	5.4e-05	2.1e-04	2.7e-04	3.5e-04	3.4e-04	3.4e-04	3.9e-04	4.7e-04	4.1e-04	1.6e-03	1.8e-03	2.2e-03	2.1e-03	5.2e-03	6.3e-03	7.6e-03	7.3e-03
congress-bills	1.9e-04	9.2e-04	3.0e-04	2.5e-04	7.6e-04	3.0e-03	1.2e-03	1.3e-03	9.9e-04	2.4e-03	1.2e-03	9.1e-04	4.2e-03	1.2e-02	5.4e-03	8.1e-03	5.4e-03	1.0e-02	5.2e-03	6.1e-03	5.0e-03	7.2e-03	3.4e-03	3.8e-03
congress-committees	0.0e+00	1.5e-04	3.7e-05	5.8e-05	0.0e+00	6.7e-04	2.9e-04	3.6e-04	0.0e+00	9.9e-04	5.7e-04	6.3e-04	0.0e+00	2.4e-03	1.5e-03	1.7e-03	0.0e+00	3.2e-03	2.2e-03	2.1e-03	0.0e+00	3.4e-03	3.0e-03	3.1e-03
email-Eu	8.2e-06	1.5e-05	1.4e-05	8.4e-06	1.3e-04	1.8e-04	1.4e-04	8.3e-05	3.3e-04	3.6e-04	5.0e-04	2.4e-04	1.7e-03	1.1e-03	1.2e-03	1.0e-03	3.6e-03	3.3e-03	3.9e-03	2.4e-03	7.8e-03	6.4e-03	8.1e-03	5.2e-03
email-Enron	6.3e-04	4.3e-04	3.8e-04	3.4e-04	5.4e-03	2.2e-03	1.8e-03	1.9e-03	4.1e-03	4.3e-03	3.3e-03	3.1e-03	1.9e-02	1.1e-02	1.5e-02	9.4e-03	2.4e-02	2.6e-02	2.3e-02	1.2e-02	2.4e-02	3.9e-02	2.5e-02	2.1e-02
contact-high-school	6.4e-07	1.1e-06	1.1e-06	9.4e-07	1.5e-05	1.6e-05	7.5e-06	1.2e-05	5.3e-05	4.3e-05	8.6e-05	3.7e-05	3.8e-04	0.0e+00	9.1e-05	7.2e-05	1.1e-03	4.1e-04	6.7e-04	3.5e-04	2.4e-03	1.6e-03	2.1e-03	1.4e-03
contact-primary-school	2.6e-06	0.0e+00	3.2e-05	1.0e-06	3.7e-06	1.7e-05	6.9e-05	3.2e-06	6.7e-05	5.6e-05	3.2e-04	1.0e-04	9.0e-05	0.0e+00	1.9e-04	5.1e-05	2.7e-04	2.6e-04	8.6e-04	2.6e-04	1.4e-03	9.9e-04	2.1e-03	8.8e-04

																
	40	60	80	100	40	60	80	100	40	60	80	100	40	60	80	100
coauth-DBLP	8.3e-03	8.6e-03	8.5e-03	7.6e-03	1.0e-02	1.1e-02	1.1e-02	1.1e-02	1.2e-02	1.5e-02	1.5e-02	1.7e-02	1.3e-02	1.6e-02	1.7e-02	1.9e-02
coauth-MAG-Geology	8.6e-03	1.2e-02	9.4e-03	1.0e-02	1.4e-02	2.0e-02	1.5e-02	1.7e-02	1.7e-02	2.9e-02	2.3e-02	2.7e-02	2.2e-02	3.7e-02	3.0e-02	4.0e-02
coauth-MAG-History	1.7e-03	3.4e-03	1.6e-03	1.9e-03	6.0e-03	9.1e-03	4.9e-03	3.8e-03	8.3e-03	2.1e-02	1.4e-02	9.1e-03	5.1e-03	3.6e-02	3.8e-02	1.5e-02
music-rap-genius	1.4e-03	2.3e-03	1.3e-03	1.1e-03	4.8e-03	2.9e-03	2.8e-03	2.2e-03	1.2e-02	7.9e-03	6.5e-03	4.6e-03	2.0e-02	1.7e-02	1.2e-02	8.6e-03
tags-stack-overflow	9.2e-05	7.0e-05	6.5e-05	6.5e-05	5.2e-04	4.4e-04	4.0e-04	3.9e-04	2.7e-03	2.3e-03	2.1e-03	2.1e-03	9.6e-03	8.4e-03	7.7e-03	7.6e-03
tags-math-sx	6.3e-04	5.6e-04	5.4e-04	5.6e-04	2.4e-03	2.3e-03	2.3e-03	2.1e-03	1.0e-02	9.1e-03	9.2e-03	8.6e-03	2.9e-02	2.7e-02	2.7e-02	2.6e-02
tags-ask-ubuntu	5.3e-04	4.5e-04	3.3e-04	2.9e-04	2.2e-03	2.2e-03	1.8e-03	1.7e-03	6.9e-03	7.1e-03	5.9e-03	5.9e-03	2.1e-02	2.3e-02	1.8e-02	1.9e-02
threads-stack-overflow	9.6e-06	6.1e-06	5.7e-06	4.9e-06	4.2e-05	3.5e-05	2.6e-05	2.5e-05	1.5e-04	1.3e-04	1.1e-04	1.1e-04	6.9e-04	5.8e-04	4.3e-04	4.7e-04
threads-math-sx	6.3e-05	5.9e-05	4.3e-05	4.0e-05	1.8e-04	2.3e-04	2.0e-04	1.7e-04	4.6e-04	6.4e-04	6.1e-04	5.4e-04	1.3e-03	2.3e-03	2.7e-03	2.2e-03
threads-ask-ubuntu	0.0e+00	0.0e+00	0.0e+00	8.4e-05	4.5e-05	9.2e-05	3.8e-04	2.9e-04	0.0e+00	5.2e-04	1.7e-03	6.5e-04	1.4e-03	2.2e-03	5.7e-03	3.6e-03
NDC-substances	1.5e-02	1.1e-02	7.6e-03	2.1e-03	3.1e-02	2.2e-02	1.3e-02	3.8e-03	4.8e-02	3.5e-02	2.2e-02	7.2e-03	7.3e-02	4.8e-02	3.9e-02	1.5e-02
NDC-classes	0.0e+00	0.0e+00	0.0e+00	0.0e+00	0.0e+00	0.0e+00	1.1e-01	0.0e+00	0.0e+00	1.3e-01	9.1e-02	5.2e-02	3.6e-02	0.0e+00	8.7e-02	3.4e-02
DAWN	1.7e-03	1.5e-03	2.3e-03	1.7e-03	5.7e-03	6.0e-03	7.9e-03	7.2e-03	1.5e-02	1.7e-02	2.2e-02	2.1e-02	4.8e-02	5.5e-02	7.3e-02	6.9e-02
congress-bills	7.9e-03	1.9e-02	9.5e-03	1.7e-02	9.5e-03	1.8e-02	1.1e-02	1.4e-02	8.4e-03	1.6e-02	1.0e-02	1.1e-02	9.6e-03	1.3e-02	1.1e-02	9.3e-03
congress-committees	0.0e+00	9.8e-03	6.1e-03	5.5e-03	0.0e+00	1.2e-02	8.5e-03	5.9e-03	0.0e+00	1.4e-02	1.1e-02	8.4e-03	0.0e+00	1.2e-02	1.6e-02	1.2e-02
email-Eu	2.5e-03	5.2e-03	1.2e-02	5.3e-03	1.6e-02	9.9e-03	1.5e-02	1.2e-02	2.6e-02	1.8e-02	2.4e-02	2.1e-02	4.7e-02	3.4e-02	4.8e-02	3.3e-02
email-Enron	0.0e+00	2.3e-02	0.0e+00	0.0e+00	6.6e-02	3.9e-02	7.6e-02	3.1e-02	5.9e-02	9.9e-02	8.2e-02	4.8e-02	9.2e-02	8.0e-02	1.4e-01	5.5e-02
contact-high-school	0.0e+00	0.0e+00	0.0e+00	2.6e-03	5.2e-03	2.2e-03	4.0e-03	1.8e-03	7.9e-03	4.9e-03	7.9e-03	5.7e-03	1.3e-02	1.2e-02	1.5e-02	1.2e-02
contact-primary-school	0.0e+00	0.0e+00	5.6e-04	3.8e-04	1.4e-03	1.3e-03	1.3e-03	7.9e-04	3.4e-03	3.6e-03	3.2e-03	3.4e-03	1.7e-02	1.8e-02	1.7e-02	1.7e-02

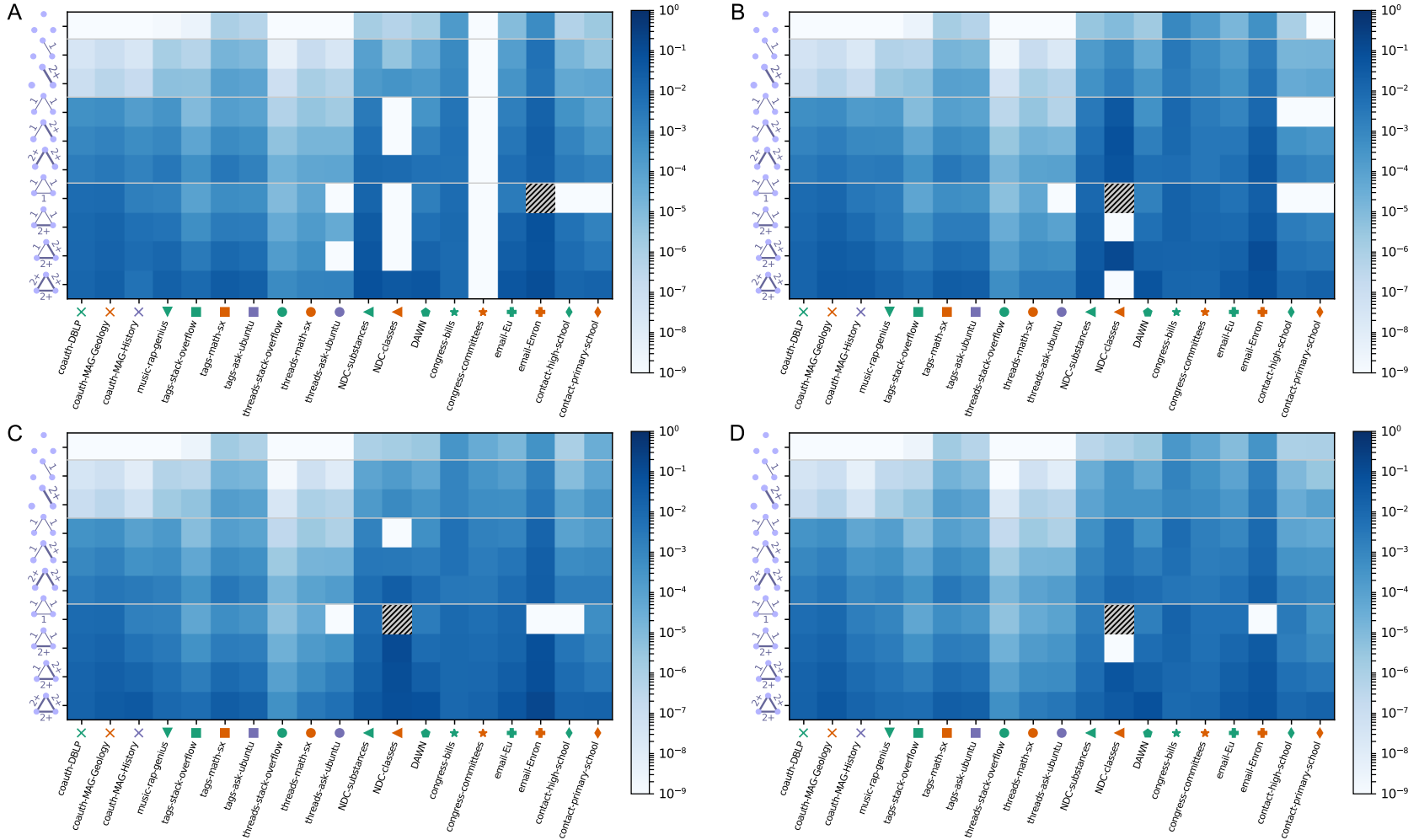


Figure 10: Heat maps of simplicial closure event probabilities of different configurations at different points in time. We first filtered each dataset to contain only the first $X\%$ of timestamped simplices, for $X = 40$ (A), $X = 60$ (B), $X = 80$ (C), and $X = 100$ (D). We then split the filtered dataset into the first 80% and last 20% of timestamped simplices (within the time frame of the filtered dataset) and compute the probability of closure in last 20% conditioned on the open configuration in the first 80%. Overall, the four heat maps of simplicial closure event probabilities exhibit similar trends (actual probabilities are listed in Table 6). Shaded boxes are cases with fewer than 25 samples. The four sections of the heat map correspond to 0, 1, 2, or 3 edges in the induced subgraph.

E EFFICIENT COUNTING OF SIMPLICIAL CLOSURE EVENT PROBABILITIES

An open configuration on three or four nodes is a set of nodes that have not jointly appeared in a simplex in the training set comprising the first 80% of the timestamped simplices (the training set). An instance of a subgraph configuration “closes” if the nodes subsequently all appear in one of the final 20% of timestamped simplices (the test set). For all newly formed simplices in the test set, we can check their prior configuration c in the training set, which provides the number of times each configuration closes. Dividing the number of closures of a configuration c by the total number of instances it was open in the training set gives the probability of a simplicial closure event. Most of the datasets we study are large enough that naively computing the simplicial closure event probabilities is infeasible. We need to develop efficient algorithms for computing the closure probabilities.

The key idea of our approach is that we do not need to *enumerate* all of the configurations in the training set and check if they close. Instead, we only need the *total count* of open configurations in the training data. We then count how many close by examining the test data directly. The idea of avoiding enumeration when simply counting suffices has been used in other fast graph configuration counting algorithms [49, 53].

E.1 Counting for 3-node configurations

We first show how to count the number of each 3-node subgraph configuration (the top row of Table 7). Recall that a weak tie corresponds to an edge in the projected graph with a weight of 1, whereas a strong tie corresponds to an edge with a weight of at least 2. Subscripts of 1 and 2 denote weak and strong ties in our notation. (Note that we use “+” for strong ties in the illustrations in Table 7; however, it will be convenient to use the integer 2 in our description of the algorithms.)

Let $\tau_{i,j,k}$, $1 \leq i \leq j \leq k \leq 2$, be the number of (open or closed) triangles whose edges have the tie strengths given by the subscripts. For instance, $\tau_{1,1,1}$ is the number of triangles whose edges are all weak ties. Similarly, let $\sigma_{i,j,k}$ be the number of triangles with given tie strengths that are open (see the right-most configurations in the first row of Table 7). We can count the number of all triangles $\tau_{i,j,k}$ using a number of efficient triangle enumeration algorithms for sparse graphs [32]. For each of these triangles we then determine whether it is closed by examining the entries of a simplex-to-node adjacency matrix (this can be efficiently read from our set-based data). The difference between the total number of triangles and the number of closed triangles gives us the open triangle counts $\sigma_{i,j,k}$.

Next, consider the number of 2-edge, 3-node induced “wedge” subgraphs. Let the symbols $\omega_{1,1}$, $\omega_{1,2}$, and $\omega_{2,2}$ denote these configurations, where the tie strengths of the two edges are given by the subscripts (see the first row of Table 7). Furthermore, let $d_1(u)$ and $d_2(u)$ be the number of weak and strong ties containing node u as an endpoint. Then $\omega_{i,j}$ is given by the number of (non-induced) 2-edge, 3-node subgraphs with tie strengths i and j minus the ones

that appear in triangles:

$$\omega_{1,1} = \sum_u \binom{d_1(u)}{2} - 3\tau_{1,1,1} - \tau_{1,1,2} \quad (4)$$

$$\omega_{2,2} = \sum_u \binom{d_2(u)}{2} - 3\tau_{2,2,2} - \tau_{1,2,2} \quad (5)$$

$$\omega_{1,2} = \sum_u d_1(u)d_2(u) - 2\tau_{1,1,2} - 2\tau_{1,2,2} \quad (6)$$

Now let η_1 and η_2 be the counts of the 1-edge, 3-node induced subgraphs, where again the tie strength of the edge is given by the subscript (see the first row of Table 7). Denote the total number of weak and strong ties by $m_s = \frac{1}{2} \sum_u d_s(u)$, $s = 1, 2$, and the total number of nodes by n . Then the total number of (non-induced) 1-edge, 3-node subgraphs with tie strength s is then $m_s(n-2)$. Induced 1-edge, 3-node subgraph are given by the non-induced counts minus the 2- and 3-edge induced counts discussed above:

$$\eta_1 = m_1(n-2) - 2\omega_{1,1} - \omega_{1,2} - 3\tau_{1,1,1} - 2\tau_{1,1,2} - \tau_{1,2,2} \quad (7)$$

$$\eta_2 = m_2(n-2) - 2\omega_{2,2} - \omega_{1,2} - 3\tau_{2,2,2} - 2\tau_{1,2,2} - \tau_{1,1,2} \quad (8)$$

Finally, let ϕ be the number of empty 3-node induced subgraphs of the projected graph (the top left of Table 7). The number of subsets of 3 nodes minus all other induced 3-node subgraphs gives the value of ϕ :

$$\phi = \binom{n}{3} - \sum_{s=1}^2 \eta_s - \sum_{1 \leq i, j \leq 2} \omega_{i,j} - \sum_{1 \leq i \leq j \leq k \leq 2} \tau_{i,j,k}. \quad (9)$$

E.2 Counting for 4-node configurations

Now we describe how we compute the simplicial closure event probabilities conditioned on the 27 subgraph configurations on four nodes in Figure 9 (these are the 4-node configurations in the second through fifth rows of Table 7). Recall that the simplicial tie strength of a triangle is (i) *open* if the three nodes form an open triangle; (ii) *weak* if the three nodes have jointly appeared in exactly one simplex; or (iii) *strong* if the three nodes have jointly appeared in at least two simplices. We use subscripts 0, 1, and 2 to denote these bins.

There are 15 total 4-node, 6-edge tetrahedral subgraph configurations. Each configuration corresponds to a non-decreasing 4-tuple of the simplicial tie strengths of the four triangles in the configuration. We denote the sum of open and closed tetrahedral counts by $\rho_{i,j,k,l}$, where i, j, k , and l denote the simplicial tie strengths, and the open tetrahedral counts by $\pi_{i,j,k,l}$ ($0 \leq i \leq j \leq k \leq l \leq 2$; the 15 configurations in the bottom two row blocks of Table 7). We may count both $\rho_{i,j,k,l}$ and $\pi_{i,j,k,l}$ by enumerating 4-cliques using, e.g., the Chiba and Nishizeki algorithm [11] and checking if each 4-clique is closed or open by examining the simplex-node adjacency matrix.

Next, we consider counts of the six 4-node, 5-edge subgraph configurations $\theta_{i,j}$, where each configuration is given by a non-decreasing pair of simplicial tie strengths for the two triangles in the configuration (the third row block of Table 7). Each instance of this configuration consists of two triangles sharing one edge. We first use a fast triangle enumeration algorithm to compute matrices $Y^{(s)}$, $s \in \{0, 1, 2\}$, where $Y_{uv}^{(s)}$ is the number of triangles with simplicial tie strength s containing nodes u and v . The counts of the non-induced configuration, which we denote by $\theta'_{i,j}$, are then

Table 7: The 10 open 3-node configurations analyzed and the 27 open 4-node configurations analyzed in Figures 8 and 9. We illustrate each 4-node configuration with a projection onto two dimensions (top—the unfilled circle represents the same node) as well as a tetrahedral three-dimensional perspective figure (bottom). For each configuration, we list (i) a reference number of the configuration and (ii) our notation for the number of instances of the configuration. For 3-node configurations, the subscripts 1 and 2 denote weak and strong simplicial ties, and for 4-node configurations, the subscripts 0, 1, and 2 denote open, weak, and strong simplicial ties. We also use $\tau_{i,j,k}$ to denote the sum of counts of open and closed 3-node, triangles ($1 \leq i \leq j \leq k \leq 2$) and $\rho_{i,j,k,l}$ to denote the sum of counts of open and closed 4-node, 6-edge tetrahedral wireframe configurations ($0 \leq i \leq j \leq k \leq l \leq 2$).

1; ϕ	2; η_1	3; η_2	4; $\omega_{1,1}$	5; $\omega_{1,2}$	6; $\omega_{2,2}$	7; $\sigma_{1,1,1}$	8; $\sigma_{1,1,2}$	9; $\sigma_{1,2,2}$	10; $\sigma_{2,2,2}$
1; λ_0	2; λ_1	3; λ_2	4; ψ_0	5; ψ_1	6; ψ_2				
7; $\theta_{0,0}$	8; $\theta_{0,1}$	9; $\theta_{0,2}$	10; $\theta_{1,1}$	11; $\theta_{1,2}$	12; $\theta_{2,2}$				
13; $\pi_{0,0,0,0}$	14; $\pi_{0,0,0,1}$	15; $\pi_{0,0,0,2}$	16; $\pi_{0,0,1,1}$	17; $\pi_{0,0,1,2}$	18; $\pi_{0,0,2,2}$	19; $\pi_{0,1,1,1}$	20; $\pi_{0,1,1,2}$	21; $\pi_{0,1,2,2}$	22; $\pi_{0,2,2,2}$
23; $\pi_{1,1,1,1}$	24; $\pi_{1,1,1,2}$	25; $\pi_{1,1,2,2}$	26; $\pi_{1,2,2,2}$	27; $\pi_{2,2,2,2}$					

given by:

$$\theta'_{s,s} = \sum_{(u,v)} \binom{Y_{uv}^{(s)}}{2}, \quad s = 0, 1, 2 \quad (10)$$

$$\theta'_{i,j} = \sum_{(u,v)} Y_{uv}^{(i)} Y_{uv}^{(j)}, \quad 0 \leq i < j \leq 2. \quad (11)$$

The summations are over the edges (u, v) in the projected graph. Each non-induced instance of these subgraph configurations may correspond to a 6-edge tetrahedral configuration, and we need to adjust for these cases. Each (open or closed) 6-edge tetrahedron count $\rho_{i,j,k,l}$ contributes to the non-induced counts $\theta'_{i,j}$, $\theta'_{i,k}$, $\theta'_{i,l}$, $\theta'_{j,k}$, $\theta'_{j,l}$, and $\theta'_{k,l}$. To get the count $\theta_{i,j}$, we subtract the portion of $\theta'_{i,j}$ coming from the tetrahedra. Denote the set of valid 4-tuples of

indices for the counts $\rho_{i,j,k,l}$ by \mathcal{S} . Formally, $\mathcal{S} = \{(i, j, k, l) \mid 0 \leq i \leq j \leq k \leq l \leq 2\}$. Then $\theta_{i,j}$ is given by

$$\begin{aligned} \theta_{i,j} = \theta'_{i,j} &- \sum_{k,l : (i,j,k,l) \in \mathcal{S}} \rho_{i,j,k,l} - \sum_{k,l : (i,k,j,l) \in \mathcal{S}} \rho_{i,k,j,l} \quad (12) \\ &- \sum_{k,l : (i,k,l,j) \in \mathcal{S}} \rho_{i,k,l,j} - \sum_{k,l : (k,i,j,l) \in \mathcal{S}} \rho_{k,i,j,l} \\ &- \sum_{k,l : (k,i,l,j) \in \mathcal{S}} \rho_{k,i,l,j} - \sum_{k,l : (k,l,i,j) \in \mathcal{S}} \rho_{k,l,i,j}. \end{aligned}$$

Next, we show how to count 4-node, 4-edge subgraph configurations that contain one triangle. There are three such configurations, corresponding to the three possible simplicial ties in the triangle,

and we denote the counts by ψ_s , $s \in \{0, 1, 2\}$ (the three right-most configurations in the second row of Table 7). We again compute non-induced counts and then subtract the induced counts of subgraphs with more edges, for which we showed how to compute above. Some additional notation will be helpful for these counts. Let \mathcal{T}_s be the set of triangles with simplicial tie strength $s \in \{0, 1, 2\}$, and let a_s and b_s count how many times triangles with a particular tie strength appear in 5-edge configuration patterns and 6-edge configuration patterns:

$$a_s = \sum_{0 \leq i \leq j \leq 2} (\text{Ind}[i = s] + \text{Ind}[j = s])\theta_{i,j} \quad (13)$$

$$b_s = \sum_{(i,j,k,l) \in \mathcal{S}} (\text{Ind}[i = s] + \text{Ind}[j = s] + \text{Ind}[k = s] + \text{Ind}[l = s])\rho_{i,j,k,l}.$$

Consider a fixed triangle (u, v, w) with simplicial tie strength s . We would like to count the number of times this triangle appears in a 4-node, 4-edge subgraph configuration. Each neighbor of each of the three nodes in the triangle is either (i) the neighbor of just one node in the triangle (ii) the neighbor of exactly two nodes in the triangle, or (iii) the neighbor of all three nodes in the triangle. The first case corresponds to the induced subgraph in which we are interested, the second case to counts $\theta_{i,j}$, and the third case to counts $\rho_{i,j,k,l}$. By the inclusion-exclusion principle,

$$\psi_s = \sum_{(u,v,w) \in \mathcal{T}_s} (d_u + d_v + d_w - 6) - 2a_s - 3b_s, \quad (14)$$

where d is the degree vector of nodes in the unweighted projected graph.

Finally, we count the 4-node subgraph configuration consisting of a triangle and an isolated node (the three leftmost configurations in the second row block of Table 7). Again, we count three types of this configuration (λ_s , $s \in \{0, 1, 2\}$), one for each of the three simplicial tie strengths of the triangle. Every triangle appears in $(n - 3)$ non-induced subgraphs with an isolated node, so we only need to subtract induced subgraph counts with more edges. We already counted these above, so the counts λ_s are given by

$$\lambda_s = |\mathcal{T}_s|(n - 3) - \psi_s - a_s - b_s. \quad (15)$$

F SCORE FUNCTIONS, HIGHER-ORDER LINK PREDICTION PERFORMANCE, AND EXAMPLE PREDICTIONS

We derive algorithms for higher-order link prediction, which fall into four broad categories for determining the score $s(i, j, k)$ of a triple of nodes:

- (1) $s(i, j, k)$ depends only on the weights of the edges (i, j) , (i, k) , and (j, k) in the projected graph
- (2) $s(i, j, k)$ is based on the local neighborhood features in the projected graph such as the common neighbors of nodes i , j , and k ;
- (3) $s(i, j, k)$ comes from a random-walk-based similarity score
- (4) $s(i, j, k)$ is a learned logistic regression model in a feature-based supervised learning setting.

Several of these score functions are generalizations of traditional approaches for dyadic link prediction [34] to account for higher-order structure.

Here we introduce some notation for this section. We denote the set of simplices that node u appears in by $R(u)$; formally, $R(u) = \{S_i \mid u \in S_i\}$. The (weighted) projected graph of a dataset is the graph on node set V , where the weight of edge (u, v) is the number of simplices containing both u and v . In other words, the $|V| \times |V|$ weighted adjacency matrix W of the projected graph is defined by

$$W_{uv} = \begin{cases} |R(u) \cap R(v)| & u \neq v \\ 0 & u = v \end{cases} \quad (16)$$

Sometimes, we will only need to consider unweighted version of the projected graph, which is encoded by the adjacency matrix A with entries $A_{uv} = \min(W_{uv}, 1)$. Finally, we denote the neighbors of a node u in the projected graph by $N(u) = \{v \in V \mid W_{uv} > 0\}$.

F.1 Weights in the projected graph

We use three score functions based on the weights of the pair-wise edges in the subgraph induced by nodes i, j , and k . The motivation for these methods is that weight-based tie strength positively correlates with probabilities of simplicial closure events in an aggregate sense. Therefore, larger weights amongst the edges between nodes i, j , and k should yield larger scores. To this end, we use the following as score functions:

$$\text{the harmonic mean: } s(i, j, k) = 3/(W_{ij}^{-1} + W_{ik}^{-1} + W_{jk}^{-1}) \quad (17)$$

$$\text{the geometric mean: } s(i, j, k) = (W_{ij}W_{ik}W_{jk})^{1/3} \quad (18)$$

$$\text{the arithmetic mean: } s(i, j, k) = (W_{ij} + W_{ik} + W_{jk})/3. \quad (19)$$

As discussed in the Section 4, these functions are all special cases of the generalized mean function.

F.2 Local neighborhood features

The next set of score functions use local neighborhood features such as common neighbors of a triple of nodes. The reasoning here is that common neighborhood structure amongst a triple of nodes are positive indicators of association of the nodes; in fact, these score functions are generalizations of traditional methods used in dyadic link prediction [34]. The common neighbors score function for a triple of nodes i, j , and k is the number of nodes that have

appeared in at least one simplex with each of the three nodes in the candidate set:

$$\text{3-way common neighbors: } s(i, j, k) = |N(i) \cap N(j) \cap N(k)|, \quad (20)$$

where again $N(x)$ is the set of neighbors of node x in the projected graph.

The Jaccard coefficient score normalizes the number of common neighbors by the total number of neighbors of the three candidate nodes:

$$\text{3-way Jaccard coefficient: } s(i, j, k) = \frac{|N(i) \cap N(j) \cap N(k)|}{|N(i) \cup N(j) \cup N(k)|}. \quad (21)$$

This score function has been used as a general multi-way similarity measurement for binary vectors [26], but has not been employed for a link prediction task until now.

Adamic and Adar proposed log-scaled normalization for features of common neighbors between two nodes [1]. Here we adapt this to a score that performs the same normalization over the common neighbors of three nodes:

$$\text{3-way Adamic-Adar: } s(i, j, k) = \sum_{l \in N(i) \cap N(j) \cap N(k)} \frac{1}{\log|N(l)|}. \quad (22)$$

Prior studies on the evolution of coauthorship have suggested preferential attachment (PA)—in terms of degree in the coauthorship network—as a mechanism for dyadic link formation [7, 42]. We use two scores based on a preferential attachment model of link formation: first is

$$\text{projected graph degree based PA: } s(i, j, k) = |N(i)| \cdot |N(j)| \cdot |N(k)| \quad (23)$$

$$\text{simplicial degree based PA: } s(i, j, k) = |R(i)| \cdot |R(j)| \cdot |R(k)|. \quad (24)$$

F.3 Paths and random walks

The next set of scores functions are path-based metrics that ascribe higher scores when there are more paths in the projected graph between a candidate triple of nodes. Recall that A and W are the unweighted and weighted adjacency matrices for the projected graph of a dataset.

The Katz score between two nodes is the sum of geometrically damped length- l paths between two nodes [27]. Katz scores have been used as a criterion for predicting dyadic links [34, 65]. Formally, the Katz score between two nodes i and j in the unweighted projected graph is $\sum_{l=1}^{\infty} \beta^l A_{ij}^l$, where β is the damping parameter and A_{ij}^l counts the number of length- l paths between i and j . All pairwise Katz scores can be computed in matrix form as:

$$K^{(u)} = (I - \beta A)^{-1} - I. \quad (25)$$

In order to guarantee that the weighted sum of length- l path lengths converges, we require that $\beta < 1/\sigma_1(A)$, the principal singular value of A (this guarantees that $I - \beta A$ is nonsingular). We chose $\beta = \frac{1}{4\sigma_1(A)}$ in our experiments.

We can also use paths in the original (weighted) projected graph, where W_{ij}^l is the number of length- l paths between i and j if we interpret the integer weights in W to be parallel edges. This leads to the weighted pairwise Katz scores

$$K^{(w)} = (I - \beta W)^{-1} - I. \quad (26)$$

Again, β must be less than $1/\sigma_1(W)$ to guarantee that $(I - \beta W)$ is nonsingular, and we choose $\beta = \frac{1}{4\sigma_1(W)}$ in our experiments.

Given the pairwise Katz scores, we define score functions for triples of nodes as follows:

$$\text{unweighted 3-way Katz: } s(i, j, k) = K_{ij}^{(u)} + K_{ik}^{(u)} + K_{jk}^{(u)} \quad (27)$$

$$\text{weighted 3-way Katz: } s(i, j, k) = K_{ij}^{(w)} + K_{ik}^{(w)} + K_{jk}^{(w)}. \quad (28)$$

For many of our datasets, storing the K matrices in a dense format requires too much memory. In these cases, we use the Krylov subspace method MINRES [47] to solve the linear systems

$$(I - \beta A)k_j = e_j, \quad j = 1, \dots, |V|, \quad (29)$$

where e_j is the j th standard basis vector. After computing k_j , we store only the entries of the j th column of K corresponding to the sparsity pattern of the j th column of A . These are the only entries of K needed for computing the scores in Eq. (27).

The personalized PageRank (PPR) score is another path-based score used in dyadic link prediction [5, 34]. PPR is based on the random walk underlying the classical PageRank ranking system for web pages [46]. More specifically, consider a Markov chain, where at each step, with probability $0 < \alpha < 1$, the chain transitions according to a random walk in a graph, and with probability $1 - \alpha$ transitions to node i . The PPR score of node j with respect to node i is then the stationary probability of the state j for the Markov chain. The PPR scores are given by the matrix

$$F^{(u)} = (1 - \alpha)(I - \alpha AD^{-1})^{-1}, \quad (30)$$

where $F_{ji}^{(u)}$ is the PPR score of j with respect to node i . Here D is the diagonal degree matrix, $D_{jj} = \sum_i A_{ij}$. We can again provide an analog for the weighted case:

$$F^{(w)} = (1 - \alpha)(I - \alpha W D_W^{-1})^{-1}, \quad (31)$$

where $[D_W]_{jj} = \sum_i W_{ij}$ is the weighted diagonal degree matrix.

As we did with the Katz scores, we construct three-way scores from the pairwise PPR scores:

unweighted 3-way PPR:

$$s(i, j, k) = F_{ij}^{(u)} + F_{ji}^{(u)} + F_{ik}^{(u)} + F_{ki}^{(u)} + F_{jk}^{(u)} + F_{kj}^{(u)} \quad (32)$$

weighted 3-way PPR:

$$s(i, j, k) = F_{ij}^{(w)} + F_{ji}^{(w)} + F_{ik}^{(w)} + F_{ki}^{(w)} + F_{jk}^{(w)} + F_{kj}^{(w)}. \quad (33)$$

(Unlike the Katz score matrices K , the PPR matrices are not symmetric, so we account for both directions of the edges.)

We also use a recent generalization of PPR scores for abstract simplicial complexes, based on tools from algebraic topology [58]. Here, we describe the computations necessary for these scores, assuming a basic knowledge of algebraic topology.

We consider the abstract simplicial complex defined by the union of the set of closed triangles T , the set of edges E , and the set of vertices V . We orient the edges and triangles so that (i, j) for $i < j$ corresponds to an edge $\{i, j\}$ and (i, j, k) for $i < j < k$ corresponds to a closed triangle $\{i, j, k\}$. Following the ideas of Schaub et al., we define the normalized combinatorial Hodge Laplacian as

$$\hat{\Delta} = (GD^{-1}G^T + C^T C)M^{-1}, \quad (34)$$

where the ‘‘gradient operator’’ G is a $|E| \times |V|$ matrix defined by

$$G_{(i,j),x} = \begin{cases} 1 & x = j \\ -1 & x = i \\ 0 & \text{otherwise,} \end{cases} \quad (35)$$

the ‘‘curl operator’’ C is a $|T| \times |E|$ matrix defined by

$$C_{(i,j,k),(x,y)} = \begin{cases} 1 & (x, y) = (i, j) \text{ or } (x, y) = (j, k) \\ -1 & (x, y) = (i, k) \\ 0 & \text{otherwise,} \end{cases} \quad (36)$$

D is a diagonal matrix defined by

$$D_{xx} = \sum_{(i,j)} |G_{(i,j),x}|, \quad (37)$$

and M is a diagonal matrix defined by

$$M_{(x,y),(x,y)} = 2 + \sum_{(i,j,k)} |C_{(i,j,k),(x,y)}|. \quad (38)$$

The matrix $P = \frac{1}{2}(I - \hat{\Delta})$ defines a Markov-like operator. The simplicial PageRank scores (defined on each pair of edges) can thus be defined analogously to the standard PageRank:

$$S = (I - \alpha P)^{-1}(1 - \alpha). \quad (39)$$

Here, the matrix S defines pairwise scores between *edges*, and we construct a score function on triples of nodes by taking the sum of pairwise scores:

3-way simplicial PPR:

$$s(i, j, k) = |S_{(i,j),(j,k)}| + |S_{(j,k),(i,j)}| + |S_{(i,j),(i,k)}| \\ + |S_{(i,k),(i,j)}| + |S_{(j,k),(i,k)}| + |S_{(j,k),(i,k)}|. \quad (40)$$

F.4 Supervised learning

Finally, we used a supervised machine learning approach that learns the appropriate score function given features of the open triangle. To this end, we further divide the training data into a sub-training set (simplices appearing in the first 60% of the entire dataset) and a validation set (simplices appearing between the 60th and 80th percentile of the time spanned by the entire dataset). We trained an ℓ_2 -regularized logistic regression model using the scikit learn library¹¹ [52] for predicting closure on the validation set using features of open structures in the sub-training set. The features for each open triangle (i, j, k) were

- (1) the number of simplices containing pairs of nodes i and j , i and k , and j and k ;
- (2) the degree of nodes i, j , and k in the projected graph: $|N(i)|$, $|N(j)|$, and $|N(k)|$;
- (3) the number of simplices containing nodes i, j , and k : $|R(i)|$, $|R(j)|$, and $|R(k)|$;
- (4) the number of common neighbors in the projected graph of nodes i and j , i and k , and j and k : $|N(i) \cap N(j)|$, $|N(i) \cap N(k)|$, and $|N(j) \cap N(k)|$;
- (5) the number of common neighbors of all three nodes i, j , and k in the projected graph: $|N(i) \cap N(j) \cap N(k)|$
- (6) the log of the features in Items 1 to 3 and the log of the sum of 1 and the feature value for the features in Items 4 and 5.

¹¹<http://scikit-learn.org/>

Table 8: Open triangle closure prediction performance based on several score functions: random (Rand.); harmonic, geometric, and arithmetic means of the 3 edge weights; 3-way common neighbors (Common); 3-way Jaccard coefficient (Jaccard); 3-way Adamic-Adar (A-A); projected graph degree and simplicial degree preferential attachment (PGD-PA and SD-PA); unweighted and weighted Katz similarity (U-Katz and W-Katz); unweighted and weighted personalized PageRank (U-PPR and W-PPR); simplicial personalized PageRank (S-PPR; missing entries are cases where computations did not finish within 2 weeks); and a feature-based supervised model using logistic regression (Log. reg.). Performance is AUC-PR relative to the random baseline. The random baseline is listed in absolute terms and equals the fraction of open triangles that close. The harmonic and geometric means of edge weights perform well across many datasets, further highlighting the role of tie strength in predicting simplicial closure events. This signal from local structure contrasts from traditional pairwise link prediction, where longer paths are needed for effective prediction [34]. The supervised method also performs well, suggesting that combinations of features capture the rich variety of structure observed across datasets.

Dataset	Rand.	Harm. mean	Geom. mean	Arith. mean	Common	Jaccard	A-A	PGD-PA	SD-PA	U-Katz	W-Katz	U-PPR	W-PPR	S-PPR	Log. reg.
coauth-DBLP	1.68e-03	1.49	1.59	1.50	1.33	1.84	1.60	0.74	0.74	0.97	1.51	1.62	1.83	1.21	3.37
coauth-MAG-History	7.16e-04	1.69	2.72	3.20	5.11	2.24	5.82	1.50	2.49	6.30	3.40	1.66	1.88	1.35	6.75
coauth-MAG-Geology	3.35e-03	2.01	1.97	1.69	2.43	1.84	2.71	1.31	0.97	1.99	1.74	1.06	1.26	0.94	4.74
music-rap-genius	6.82e-04	5.44	6.92	1.98	1.85	1.62	2.10	1.82	2.15	1.93	2.00	1.78	2.09	1.39	2.67
tags-stack-overflow	1.84e-04	13.08	10.42	3.97	6.45	9.43	6.63	3.37	2.74	2.95	3.60	1.08	1.85	-	3.37
tags-math-sx	1.08e-03	9.08	8.67	2.88	6.19	9.37	6.34	3.48	2.81	4.53	2.71	1.19	1.55	1.86	13.99
tags-ask-ubuntu	1.08e-03	12.29	12.64	4.24	7.15	4.96	7.51	7.48	5.63	7.10	4.15	1.75	2.54	1.19	7.48
threads-stack-overflow	1.14e-05	23.85	31.12	12.97	2.73	3.85	3.19	5.20	3.89	1.06	11.54	1.66	4.06	-	1.53
threads-math-sx	5.63e-05	20.86	16.01	5.03	25.08	28.13	23.32	10.46	7.46	11.04	4.86	0.90	1.18	0.61	47.18
threads-ask-ubuntu	1.31e-04	78.12	80.94	29.00	21.04	2.80	30.82	7.09	6.62	16.63	32.31	0.94	1.51	1.78	9.82
NDC-substances	1.17e-03	4.90	5.27	2.90	5.92	3.36	5.97	4.76	4.46	5.35	2.93	1.39	1.83	1.86	8.17
NDC-classes	6.72e-03	4.43	3.38	1.82	1.27	1.19	0.99	0.94	2.14	0.92	1.34	0.78	0.91	2.45	0.62
DAWN	8.47e-03	4.43	3.86	2.13	4.73	3.76	4.77	3.76	1.45	4.61	2.04	1.57	1.37	1.55	2.86
congress-committees	6.99e-04	3.59	3.28	2.48	4.83	2.49	5.04	1.06	1.31	3.21	2.59	1.50	3.89	2.13	7.67
congress-bills	1.71e-04	0.93	0.90	0.88	0.65	1.23	0.66	0.60	0.55	0.60	0.78	3.16	1.07	6.01	107.19
email-Enron	1.40e-02	1.78	1.62	1.33	0.85	0.83	0.87	1.27	0.83	0.99	1.28	3.69	3.16	2.02	0.72
email-Eu	5.34e-03	1.98	2.15	1.78	1.28	2.69	1.37	0.88	1.55	1.01	1.79	1.59	1.75	1.26	3.47
contact-high-school	2.47e-03	3.86	4.16	2.54	1.92	3.61	2.00	0.96	1.13	1.72	2.53	1.39	2.41	0.78	2.86
contact-primary-school	2.59e-03	5.63	6.40	3.96	2.98	2.95	3.21	0.92	0.94	1.63	4.02	1.41	4.31	0.93	6.91

After learning the model, we predicted on the test set using the same features computed on the entire training set (first 80% of the dataset).

F.5 Prediction performance

Using the ranking induced by the score functions described above, we evaluated the prediction performance on each dataset by the area under the precision-recall curve (AUC-PR) metric (Table 8). We use random scores—more specifically, a random ranking—as a baseline, and report scores relative to this baseline.

As seen in Section 4, our proposed algorithms can achieve much higher performance than randomly guessing which open triangles go through a simplicial closure event. We also still see good performance of the harmonic and geometric means, as well as the supervised problem, with respect to this expanded set of score functions.

We may further decompose the pairwise scores of simplicial PageRank scores in Eq. (40) into the gradient, harmonic, and curl components given by the Hodge decomposition [58]. Computationally, we solve the least squares problems

$$\min_X \|GX - S\|_F, \quad \min_Y \|C^T Y - S\|_F \quad (41)$$

using the iterative method LSQR [48] (with tolerances 10^{-3}) on each column. Given the minimizers X^* and Y^* of Eq. (41), the components of the Hodge decomposition are

$$S_{\text{grad}} = GX^*, \quad S_{\text{curl}} = C^T Y^*, \quad S_{\text{harm}} = S - S_{\text{grad}} - S_{\text{curl}}. \quad (42)$$

Each of S_{grad} , S_{curl} , and S_{harm} defines pairwise scores between edges, and we construct score functions on triples of nodes in the same way as in Eq. (40).

We report the performance results in Table 9 for the datasets that were small enough on which computing the Hodge decomposition was computationally feasible. We observe that the components from the Hodge decomposition can provide substantially better results than the “combined” simplicial PageRank score reported Table 8. However, no component consistently out-performs the others.

F.6 Example predictions

Lastly, we provide a concrete example of predictions. Table 10 shows the top 25 predictions of the Adamic-Adar score function on the DAWN dataset. In this dataset, fewer than one in a hundred open triangles in the training set experience a simplicial closure event in the test set, but 4 of the top 25 predictions from this score function go through a simplicial closure event. Three of the correct predictions relate to novel combinations with proton pump inhibitors.

Table 9: Open triangle closure prediction performance based on score functions from the Hodge decomposition of the simplicial personalized PageRank vector.

Dataset	Rand.	combined	gradient	harmonic	curl
coauth-MAG-History	7.16e-04	1.35	1.25	1.13	1.27
music-rap-genius	6.82e-04	1.39	1.44	1.40	1.47
tags-math-sx	1.08e-03	1.86	0.73	0.66	0.74
tags-ask-ubuntu	1.08e-03	1.19	0.61	0.59	0.71
threads-ask-ubuntu	1.31e-04	0.61	0.58	0.61	4.59
NDC-substances	1.17e-03	1.86	0.63	0.72	0.60
NDC-classes	6.72e-03	2.45	1.37	0.83	1.74
DAWN	8.47e-03	1.55	0.59	0.60	0.65
congress-committees	6.99e-04	2.13	1.22	1.13	1.63
email-Enron	1.40e-02	2.02	2.90	1.98	2.46
email-Eu	5.34e-03	1.26	1.28	0.82	1.63
contact-high-school	2.47e-03	0.78	0.99	1.68	2.38
contact-primary-school	2.59e-03	0.93	1.45	1.84	3.26

Table 10: Top 25 predictions from the 3-way Adamic-Adar algorithm for open triangles to go through a simplicial closure event in the DAWN dataset. An “X” marks open triangles that actually go through a simplicial closure event final 20% of the time spanned by the dataset. Four of the top 25 predictions do indeed have a simplicial closure event.

1	methyldopa; gentamicin; proton pump inhibitors
2	X norepinephrine; chlormezanone; proton pump inhibitors
3	ranitidine; gentamicin; proton pump inhibitors
4	dihydroergotamine; methyldopa; asa/butalbital/caffeine/codeine
5	ranitidine; gentamicin; levodopa
6	praziquantel; diazepam; alfentanil
7	asa/caffeine/dihydrocodeine; praziquantel; proton pump inhibitors
8	chloral hydrate; tobramycin; sumatriptan
9	oxybutynin; gentamicin; tobramycin
10	asa/caffeine/dihydrocodeine; norepinephrine; sumatriptan
11	ampicillin; chlormezanone; proton pump inhibitors
12	bepidil; diazepam; alfentanil
13	colestipol; oxybutynin; proton pump inhibitors
14	X nadolol; benazepril; proton pump inhibitors
15	thalidomide; amiloride; maprotiline
16	X nadolol; lamivudine-zidovudine; proton pump inhibitors
17	chloral hydrate; verapamil; methyldopa
18	chlorzoxazone; benazepril; proton pump inhibitors
19	heparin; asa/caffeine/dihydrocodeine; proton pump inhibitors
20	oxcarbazepine; norepinephrine; proton pump inhibitors
21	dihydroergotamine; tobramycin; alfentanil
22	maprotiline; norepinephrine; proton pump inhibitors
23	oxybutynin; methyldopa; dihydroergotamine
24	heparin; dihydroergotamine; proton pump inhibitors
25	X ampicillin; methyldopa; diazepam